HHS Public Access

Author manuscript

Biochim Biophys Acta. Author manuscript; available in PMC 2017 June 01.

Published in final edited form as:

Biochim Biophys Acta. 2016 June ; 1862(6): 1214–1227. doi:10.1016/j.bbadis.2016.02.003.

Human βA3/A1-crystallin splicing mutation causes cataracts by activating the unfolded protein response and inducing apoptosis in differentiating lens fiber cells

Zhiwei Ma[1], **Wenliang Yao**[1,2], **Chi Chao Chan**[3], **Chitra Kannabiran**[1,4], **Eric Wawrousek**[5], and **J. Fielding Hejtmancik**[1,6]

[1]Ophthalmic Genetics and Visual Function Branch, National Eye Institute, National Institutes of Health, Bethesda, MD, USA

[2]Medimmune, Gaithersburg, MD

[3]Histology Core, National Eye Institute, NIH

[4]Kallam Anji Reddy Molecular Genetics Laboratory, L.V. Prasad Eye Institute, Hyderabad, Andhra Pradesh, India

[5]Laboratory of Molecular and Developmental Biology, National Eye Institute, NIH

Abstract

βγ-Crystallins, having a uniquely stable two domain four Greek key structure, are crucial for transparency of the eye lens,. Mutations in lens crystallins have been proposed to cause cataract formation by a variety of mechanisms most of which involve destabilization of the protein fold. The underlying molecular mechanism for autosomal dominant zonular cataracts with sutural opacities in an Indian family caused by a c.215+1G>A splice mutation in the βA3/A1-crystallin gene CRYBA1 was elucidated using three transgenic mice models. This mutation causes a splice defect in which the mutant mRNA escapes nonsense mediated decay by skipping both exons 3 and 4. Skipping these exons results in an in-frame deletion of the mRNA and synthesis of an unstable p.Ile33_Ala119del mutant βA3/A1-crystallin protein. Transgenic expression of mutant βA3/A1-crystallin but not the wild type protein results in toxicity and abnormalities in the maturation and orientation of differentiating lens fibers in c.97_357del CRYBA1 transgenic mice, leading to a small spherical lens, cataract, and often lens capsule rupture. On a cellular level, the lenses accumulated p.Ile33_Ala119del βA3/A1-crystallin with resultant activation of the stress signaling pathway- Unfolded Protein Response (UPR) and inhibition of normal protein synthesis, culminating in apoptosis. This highlights the mechanistic contrast between mild mutations that destabilize crystallins and other proteins, resulting in their being bound by the α-crystallins that buffer lens cells against damage by denatured proteins, and severely misfolded proteins that are

[6]Corresponding author: J. Fielding Hejtmancik, M.D., Ph.D., OGVFB/NEI/NIH, 5635 Fishers lane, Room 1127, Rockville, MD, 20852, Phone: 301-496-8300, Fax: 301-435-1598, f3h@helix.nih.gov.

not bound by α-crystallin but accumulate and have a direct toxic effect on lens cells, resulting in early onset cataracts.

Keywords

Splice Mutation; Cataract; Crystallin gene; Unfolded Protein Response; Apoptosis

Introduction

Crystallins are highly abundant structural proteins critical for the optic properties of the lens (Hejtmancik et al. 2001). Their expression increases from the anterior epithelial cells to the terminally differentiated fiber cells, where they make up over 90% of soluble lens proteins. The stability, high concentrations, and short-range ordered packing of the crystallins are important for the maintenance of lens transparency and refractive power. Three major families of ubiquitous crystallins, α, β, and γ, are expressed in all vertebrate lenses. Of these, the βγ-crystallins form a large gene family with related Greek key motif structures. The β-crystallin family can be divided into more acidic (βA-) and more basic (βB-) crystallins, of which each subgroup is encoded by three genes (CRYBA1, −2, and −4; CRYBB1, −2, and −3). CRYBA1 encodes two proteins (βA3-crystallin and βA1-crystallin) from a single mRNA. The latter protein, which is generated by use of an alternate translation initiation site, is 17 amino acids shorter than βA3-crystallin. This feature is conserved among all mammals, birds, and frogs.

Mutations in β-Crystallin genes, *CRYBA1, CRYBA2, CRYBA4, CRYBB1, CRYBB2, and CRYBB3* have been reported to cause dominant cataracts in humans (Shiels et al. 2010). CRYAA, CRYAB, *CRYBB1* and *CRYBB3* have been associated with recessive cataracts, suggesting that they might have a function in addition to their role as structural lens proteins (Cohen et al. 2007; Khan et al. 2007; Meyer et al. 2009; Pras et al. 2000; Riazuddin et al. 2005; Safieh et al. 2009). However, most identified mutations in lens crystallins cause autosomal dominant cataracts, consistent with their role as structural proteins. The dominant inheritance pattern presumably reflects a gain of deleterious function or characteristic in the mutant protein. Possible lens and extralenticular functions are being gradually suggested for the crystallins (Sinha et al. 2008). However, it is certain that β-crystallins play a vital role in lens development and the maintenance of lens transparency (Hejtmancik et al. 2001). Although some β-crystallins appear to have calcium binding activity (Jobby and Sharma 2007), the only biochemical or enzymatic activity identified in a member of the β/γ-crystallin superfamily to date is the detergent-activated proteolytic activity of βA3/A1-crystallin (Srivastava and Srivastava 1996).

Mutations in βA3/A1-crystallin are well known to cause cataract formation in both humans and mice (see the Cat-Map database, (Shiels et al. 2010)). In particular, mutations altering the 5′ (donor) splice sequence of exon 3 have been reported in multiple families with autosomal dominant cataracts (Bateman et al. 2000; Burdon et al. 2004; Devi et al. 2008; Gu et al. 2010; Kannabiran et al. 1998; Sun et al. 2011; Yang et al. 2011; Yang et al. 2012; Yu et al. 2012; Zhu et al. 2010). While identification of identical or functionally similar splice

mutations in these families of various ethnic backgrounds has provided strong support for the causality of these splice mutations, the mechanism through which they act remained unclear. This is particularly so since splice or nonsense mutations in internal exons resulting in premature termination of protein synthesis usually result in nonsense mediated decay of the mutant mRNA and absence of the encoded protein rather than synthesis of an aberrant protein product. In this regard, no recessive cataracts currently have been described as a result of mutations in βA3/A1-crystallin, all of which are dominant. Similarly, to date, cataracts have not been demonstrated to result from haploinsufficiency of a lens crystallin.

We previously described an Indian family with autosomal dominant cataracts having both a zonular component in the fetal nucleus and uniform prominent opacities of both the anterior and posterior Y-sutures in the area enclosed by the zonular component (Basti et al. 1996). We mapped the cataract locus with a lod score of 3.91 to a region of chromosome 17q11-q12 including the βA3/A1-crystallin gene and identified a c.215+1G>A mutation in the CRYBA1 gene that was predicted to inactivate splicing (Kannabiran et al. 1998). The current study characterizes the *in vivo* effects of the c.215+1G>A splice mutation of βA3/A1–crystallin in the lens and in a cultured lens cell line. Transgenic expression of human CRYBA1 with this splice mutation is shown to result in production of an mRNA skipping both exons 3 and 4 and yielding an in frame deletion in the mutant protein. Transgenic expression of the resulting p.Ile33_Ala119del βA3/A1 mutant crystallin protein caused severe alterations of cellular structure of the lens and cataracts. These cataracts are associated with induction of the UPR as indicated by increased expression of BiP/GRP78 and other UPR components in mice transgenic for the p.Ile33_Ala119del βA3/A1 mutant crystallin, activating apoptosis pathways and causing the resultant lens opacity in c.97_357del CRYBA1 transgenic mice.

Materials and Methods

Transgenic mice

Mice transgenic for the 7.5 kb CRYBA1 gene (NG_008037.1) were generated by PCR of genomic DNA from affected individual 1384 using primers: 1201 (5′ GCGGAATTCGTGGTACCAGATGGAGACCCAG3′) located at positions c.-10-12 with an EcoRI site included, and 1202 (5′ CATGCTTGAGGAATTATCG3) located at positions c.648+21-39′ of the human CRYBA1 gene (Fig. 1A). The EcoRI compatible restriction sites were used to clone the PCR product into PACP2, an expression vector incorporating the chicken α-crystallin promoter and an SV40 splice and polyA site in a pT7 plasmid backbone (Fig. 1B). The insert, including 412bp CRYAA minimal promoter (Chepelinsky et al. 1985), and the SV40 small-t antigen intron splice and poly(A) region (Chepelinsky et al. 1985) was then excised with NotI and used to construct transgenic mouse lines. Transgenic mice were generated by pronuclear microinjection of the purified fragments into pronuclear stage inbred FVB/N embryos as described by Wawrousek et al.(Wawrousek et al. 1990). Transgenic mice were screened by polymerase chain reaction (PCR) from tail genomic DNA, using primers 1221 (5′ GCTAGCTCACCACCGCACTGCC 3′), 1227 (5′ AAGGAGAGGAAGGGCAAGGG3′). The p.Ile33_Ala119del mutant cDNA was isolated from lenses of mice transgenic by RT-PCR using 5′

GAATTCATGGAGACCCAGGCTGAGCA3′ and 5′GAATTCCTACTGTTGGATTCGGCG. All constructs were confirmed by bidirectional Sanger sequencing.

The structure of the c.215+1G>A mRNA (NM_005208.4) was elucidated by reverse transcription PCR (RT-PCR) using primers 1274 (5′ATGGAGACCCAGGCTGAGCA3′) located at position c.1-20 (encoded by exon 1) and 1294 (5′GGCTCAGACCAACCCTACGC3′) located at position c.54-73 (encoded by exon 2) as forward primers for PCR amplifications, and primers 1295 (5′CACTCCAAGGCATCCCAGCGA3′) located at position c.282-301 (encoded by exon 4) and 1271 (5′GCCCCACTCTCTCCAATGTTTATAG3′) located at positions c.573-597 (encoded by exon 6) for reverse primers. Primer 1294 (5′GGCTCAGACCAACCCTACGC3′) efficiently amplified both the mouse and human CRYBA3 exon 2 sequences, even though the corresponding mouse sequence (5′GGCTCAGACCAACCCTATGC3′) has a single base change. Direct bidirectional Sanger sequencing of PCR products was carried out using the same primers.

The wt CRYBA1 and c.97_357del (NM_005208.4) CRYBA1 mutant transgenes were constructed by cloning the full-length human βA3/A1-crystallin cDNA and the c.97_357del (p.Ile33_Ala119del) mutant βA3/A1-crystallin cDNA lacking exon3 and exon4, cloned from lenses of mice transgenic for the 7.5 kb c.215+1G>A splice mutant CRYBA1 (above) into the compatible EcoRI site of the pCBB1 vector. This vector contains the 468 bp chicken βB1-crystallin promoter (Chen et al. 2001) followed by the cloning site and then the terminal part of mouse CryBA1 exon5, intron5 and exon6, including the final splice site and the polyadenylation signal (Fig 2A) in a pNEB193 backbone. After confirming the sequence and orientation by bidirectional Sanger sequencing on an ABI 3130 Genetic analysis system (Foster City, CA), the constructs were digested by PmeI. Target fragments were purified by Agarose Gel DNA Extraction Kit (Roche). Transgenic mice were generated by pronuclear microinjection of the purified fragments into pronuclear stage inbred FVB/N embryos as described by Wawrousek et al.(Wawrousek et al. 1990).

Transgenic mice were screened by polymerase chain reaction (PCR) from tail genomic DNA, using primers derived from the chicken βB1-Crystallin promoter (Fr1: 5′-CAGCTGGGTATGCCCAAGGTG-3′) and (Re1: 5′-CAGCTGCTGCTTCTTGTTGGA-3′). A 403-bp DNA fragment was amplified and visualized by agarose gel electrophoresis and ethidium bromide staining. All studies were performed in non-transgenic and heterozygous transgenic animals, and whenever possible comparisons were made between non-transgenic and transgenic littermates. All procedures with mice in this study were performed in compliance with the tenets of the National Institutes of Health Guideline on the Care and Use Animals in research, and the ARVO Statement for the Use of Animals in Ophthalmic and Vision Research.

Morphometric analysis

Darkfield photomicrographs were obtained with a Zeiss Stemi-SV11 dissecting scope (Carl Zeiss, München, Germany). For morphometric observation, the lenses from transgenic mice at different ages were enucleated under a dissecting microscope and photographed. Images were taken of enucleated fresh lenses immersed in PBS at 37°C.

Histological analysis

Eyes from mice of different ages were enucleated and fixed overnight in 10% neutral buffered formalin. After dehydration and clarification, they were embedded in methacrylate and sectioned serially at 2μm thickness through the pupillary optic nerve axis, then stained with hematoxylin and eosin (H&E) by standard histological techniques. The sections were evaluated by light microscopy, and images were obtained by means of a scanning camera equipped with a screening-capture program (Axiocam HRC and AxioVision; Carl Zeiss)

Real-time PCR

Total RNA was extracted from lenses of transgenic and control mice of different ages using an RNA isolation kit (RNeasy plus Mini kit; Qiagen) according to the manufacture's instructions. In addition, liver, lung, spleen, heart, kidney, pancreas, testis, stomach, intestine, striated muscle, diaphragm, uterus tissues were isolated from 2-6 months mice and either stored at −80°C or processed immediately. Total RNA concentrations were estimated by spectrophotometer at 260nm, and 1 μg of each total RNA was reverse transcribed (ThermoScript RT-PCR system; Invitrogen, Carlsbad, CA) according to the manufacturer's instructions.

Quantitative real-time PCR was performed with SYBR Green kits (QIAGEN). The primers were standardized and the efficiency was tested before performing real-time PCR; primers with an efficiency above 95% were used in this study. Cycling conditions were: 95°C for 15s, 60°C for 30s, 72°C for 30s. The integrity of PCR products were verified with dissociation curve analysis to ensure no primer-dimers had formed and to check for a single amplicon. To verify the presence of a single PCR product, samples were also electrophoresed on a 2% agarose gel. The housekeeping gene Gapdh and ribosomal protein gene Rpl19 served as endogenous controls for quantitation of crystallin genes and UPR genes respectively. Relative expression was calculated following the 2^(-delta delta Ct) method. Primers are listed in Table 1.

RT^2 Profiler PCR Array

Lens RNA was purified using RNeasy Microarray Tissue Mini kit from different aged mice. cDNA was prepared from purified RNA using RT^2 First Strand kit. After adding cDNA to RT^2 SYBR Green Mastermix, aliquots were mixed into a 384 well Unfolded Protein Response RT^2 Profiler PCR Array, which profiles the expression of 84 key genes recognizing and responding to misfolded protein accumulation in the endoplasmic reticulum (ER). Real-time PCR was performed using a Life Technologies ViiA-7. After the PCR was run, the Ct values were exported and analyzed with web-based PCR array data analysis software (www.SABiosciences.com/pcrarraydataanalysis.php).

SDS-PAGE and western-blot analysis

Lenses were isolated from wild type and c.97_357del CRYBA1 transgenic mice after euthanasia, and homogenized in lysis buffer containing 1×PBS, 1mM PMSF, 1% Triton X-100, 1mM DTT and a protease inhibitor cocktail including Aprotinin, Bestatin, E-64, leupeptin and Pepstatin A (Sigma, St. Louis, MO) for 3 min at 4°C. The protein concentration was measured with a protein assay reagent (BCA; Pierce, Rockford, IL) using

BSA as a standard. Approximately 10μg of protein from each preparation was loaded on 4-12% NuPAGE Bis-Tris gels (Invitrogen). The gels were stained with Coomassie brilliant blue. For Western blotting, proteins were transferred to PVDF membranes (Bio-Rad Laboratories, Richmond, CA), blocked with blocking buffer (Roche), and incubated with rabbit polyclonal antibody to a recombinant fragment corresponding to amino acids 1 through 215 of βA3-crystallin (NOVUS, Littleton CO, cat. NBP1-33010) overnight at 4°C. HRP-conjugated anti-rabbit IgG (Promega) and 4-CN substrate (Thermo Scientific) were used for visualization.

Detection of apoptosis

In the present study, a terminal deoxynucleotidyl transferase dUTP nick end labeling (TUNEL) assay was employed to detect apoptosis. A TUNEL Apoptosis Detection Kit (DNA Fragmentation/Fluorescence Staining) was used to detect apoptosis in mice lenses after birth according to the manufacturer's instructions (Millipore)

Transcription analysis in Human Lens epithelial cells

Full length CRYBA1 was amplified from genomic DNA using four primer couples (Table 1) Four fragments were purified and cloned into a TA vector (PCR®2.1 TOPO) firstly. After confirming the sequence and orientation by sequencing on a Prism 3130 DNA Analysis System (Applied Biosystems Inc. [ABI], Foster City, CA) the target fragments were released by Kpn1, BamH1, Xba1, Nde1, and Xho1 digestion separately. Four purified fragments were inserted into digested pcDNA4/HisMax© A vector. The mutant construction was created by PCR-amplified fragments from patient genomic DNA. The wild-type and mutant plasmids were confirmed by sequencing and named as pcDNA4A/CRYBA1/WT and pcDNA4A/CRYBA1c.215+1G>A respectively.

Human lens epithelial cells (FHL124) (Wormstone et al. 2000) were maintained in Dulbecco's Modified Eagle Medium supplemented with 10% fetal bovine serum in a humidified atmosphere containing 5% CO2 at 37 °C. The expression vectors pcDNA4A/CRYBA1/WT and pcDNA4A/ CRYBA1c.215+1G>A were transfected into Human lens epithelial cells using PolyJet In Vitro DNA Transfection Reagent (SignaGen Laboratories, MD). For nonsense mediated decay studies, transfected cells were treated with 0, 5μM and10 μM PTC124 separately (Santa Cruz Biotechnology, CA) for 48h.

Human lens epithelial cells were harvested 48 h after transfection. Total cellular RNA was extracted using an RNeasy plus Mini Kit (Qiagen), and then cDNA was synthesized using a ThermoScript RT-PCR system (Invitrogen, Carlsbad, CA) according to the manufacturer's instructions. mRNA Analyses in cells were performed using primers spanning exon 1 to exon 6 (F: ATGGAGACCCAGGCTGA, R: TCTCCTCCATGATGGTCACA). The amplified products were separated by electrophoresis on 1% agarose gels.

Immunofluorescence staining

HLE cells transfected with pcDNA3,1/CRYBA1-cDNA, and pcDNA3.1/CRYBA1 c.97_357del cDNA were cultured in four well chamber slides. After 24 hours incubation, cells were fixed in freshly prepared 4% paraformaldehyde in 1× PBS for 20 min, washed twice

with PBS, and then incubated in cold blocking buffer (1% goat serum, 0.05%Tween-20, 1% BSA in 1 × PBS) overnight at 4°C. Blocking buffer was removed and cells were incubated with primary antibodies: rabbit polyclonal anti-CRYBA3 (Novus Biologicals), and mouse monoclonal anti-p62/SQSTM1 (abcam)) diluted 1:400, 1:40 respectively in 1% BSA buffer (1% bovine serum albumin, 0.05%Tween-20 in 1× PBS) for 1 hour at room temperature. After washing off the unbound first antibody, the cells were incubated in the second antibody, Alexa Fluor 488 goat-anti rabbit IgG or Alexa Fluor 555 goat-anti mouse IgG, DAPI (blue color, 1μg/ml) diluted in cold 1%BSA buffer. LysoTracker Red DND-99 antibody (Invitrogen, USA, 1:20000) was incubated with live transfected cells for 20 min according to the manufacturer's instructions. Excess buffer was removed and the cells were covered with Gel-Mount and a cover slip. Images were taken by fluorescence confocal microscopy (Zeiss LSM 700 laser scanning fluorescence confocal microscope). For confocal microscopy using wheat germ agglutinin (WGA) lens sections were rehydrated according to the following procedure: xylene for 3×3 minutes. 100% alcohol for 2×3 minutes, 90% alcohol for 1×3 minutes, 80% alcohol for 1×3 minutes, and distilled water for 4×2 minutes. Lens sections were then incubated in HBSS with 10ug/ml wheat germ agglutinin Alexa Fluor® 555 Conjugated (ThermoFisher, cat. W32464) for 30 minutes at room temperature. They were then washed twice in HBSS, and labeled with DAPI for 20 minutes. After washing twice more in HBSS, sections were covered with Gel-Mount and a cover slip. Images were taken by fluorescence confocal microscopy (Zeiss LSM 700 laser scanning fluorescence confocal microscope).

Size Exclusion Chromatography

Fifty μg of lens soluble proteins from P7D c.97_357del mutant CRYBA1 transgenic mice were loaded on an Enrich SEC650 column (Bio-Rad, Hercules, California) in running buffer: 50mM Tris-HCl, 1 mM EDTA, 0.5 M NaCl, 1mM DTT, and 50 μM TCEP. The sample was eluted with 1.25 column volumes at 0.1 ml/min and 0.5 ml fractions were collected. Aliquots of the samples were then analyzed by SDS-PAGE and western blotting as above.

Results

Expression and splice analysis of mice expressing WT and c.215+1G>A mutant CRYBA1

In order to investigate the effect of the c.215+1G>A mutation on splicing of CRYBA1 mRNA, and specifically how it escapes nonsense mediated decay, the pT7 backbone of PACP2-CRYBA1 was removed by digestion with Not I and the entire human CRYBA1 gene, driven by the 412bp CRYAA promoter and followed by a SV40 splice and PolyA site, was injected into mouse oocytes (Fig. 1A, B). Mice transgenic for WT or c.215+1G>A mutant CRYBA1 (Fig. 1A, B) showed no increase in lens opacities above background (data not shown). RT-PCR of mRNA isolated from lenses of mice transgenic for the c.215+1G>A mutant but not the wt CRYBA1 gene showed a 283 bp PCR product when primers homologous to the sequences in human exons 2 and 6 were used, but no band when primers located in human exons 2 and 4 were used, consistent with skipping of both exons 3 and 4 during splicing of the c.215+1G>A mutant gene (Fig. 1A, C). In contrast, when primers homologous to mouse exons 2 and 4 were used strong bands were seen at 248 bp in both

transgenic and control lenses (Fig. 1C). Isolation and sequencing of the amplified junctional fragments confirmed splicing directly from exon 2 to exon 5 in the c.215+1G>A mutant CRYBA1 transgenic transcript (Fig. 1D). Laemmli PAGE of an extract of soluble lens proteins displayed only the wild type crystallins from both control and transgenic mice when total proteins were stained with Coomassie Brilliant Blue (data not shown). However, Western blots of these gels showed an additional faint band at 15 kDa reacting with antibodies to the carboxyl but not the amino-terminal domains (Hope et al. 1994), consistent with predictions from the mRNA splicing results. Thus, the p.Ile33_Ala119del mutant CRYBA3/A1 protein was produced in the c.215+1G>A mutant CRYBA1 transgenic mice, but at a low level sufficient only to be detected by immunoblots but not PAGE.

Phenotype of transgenic mice

The c.215+1G>A mutant CRYBA1, which was not expressed at high levels in transgenic mice, encoded a c.97_357del CRYBA1 mRNA. This mRNA was then cloned and used as the basis of a minigene vector which should be expressed at higher levels in transgenic mice. In order to increase synthesis of the p.Ile33_Ala119del mutant CRYBA3 protein to levels more similar to those of endogenous crystallins, mice transgenic for PCBB1/ c.97_357del CRYBA1 were constructed (Fig. 2A). This vector uses a chicken CRYBB1 promoter driving the c.97_357del CRYBA1 cDNA followed by mouse Cryba1 splice and polyadenylation sites. Control mice were also constructed using the PCBB1 vector with wt CRYBA1 human cDNA. Using this vector, lens morphology was clearly affected by expression of the c. 97_357del (p.Ile33_Ala119del) mutant human βA3/A1-crystallin, with striking differences in transparency, size and shape when compared to both wild type mouse lenses and those from mice transgenic for normal human βA3/A1-crystallin (Fig 2B). The size of lenses from c.97_357del CRYBA1 transgenic mice was consistently smaller than those of wt CRYBA1 cDNA transgenic or non-transgenic mice (Fig. 2B); moreover the lenses were more spherical in shape. The posterior polar region was particularly abnormal, with bulges in the lens surface frequently seen. Finally lens opacities were formed either rapidly in severely affected mice, often with rupture of the lens posterior pole, or more gradually with accumulation of abnormal fiber cells until P16W and becoming more severe with ageing. In contrast, lenses from mice transgenic for wild-type human βA3/A1-crystallin were indistinguishable from those of age matched non-transgenic control mice.

Western Blot Analysis of the c.97_357del CRYBA1 transgenic mouse lens

To investigate whether the c.97_357del CRYBA1 transgene is effectively translated in the mouse lens, polyacrylamide gel electrophoresis and then western blot analyses were carried out on soluble and insoluble extracts of lens proteins. The c.215+1G>A mutation, located at the donor splice site for intron 3 and resulting in absence of exons 3 and 4 from the final mRNA product, is predicted to produce a p.Ile33_Ala119del 387 amino acid protein with a calculated molecule weight of 15kDa, as compared to the normal 22kDa wt mouse βA3/A1-crystallin. A band at approximately 14 kDa, consistent with the predicted size of the mutant protein, was seen in the Coomassie stained SDS-PAGE of lens water-soluble extract in the c. 97_357del CRYBA1 lane but not in the wt CRYBA1 lane (Fig. 2C). On a Western blot carried out with a polyclonal antibody against βA3/A1-crystallins (Nobus Biologicals USA), the same band at approximately 14 kDa was visualized only in the c.97_357del CRYBA1

lanes. An additional band reactive to the βA3/A1- crystallin antibody is also seen at approximately 10 kDa. In contrast, bands expected for endogenous β-crystallins, including one above 17 kDa, were seen in both the WT and mutant lens extracts. While not as heavy as the endogenous β-crystallin bands, these results confirm that the p.Ile33_Ala119del mutant βA3/A1-crystallin protein was expressed in the transgenic lenses at levels detectable by PAGE, significantly more than with the PACP derived vector. The immunoreactive band at 10 kDa increased as the lens aged, consistent with it being a degradation product of the mutant βA3/A1-crystallin protein. To further examine the fraction of mutant protein in the soluble and insoluble extracts of lens proteins, these were analyzed with Western blots from 6 months lenses from both wt and mutant transgenic mice. Essentially all the mutant protein was degraded to the 10 kDa fragment in the 6M lenses, and most of the unstable mutant protein was seen in the insoluble pellet as compared to the supernatant (Fig. 2D).

Histology of wild-type and HBA3spl transgenic mouse lenses

At E13D, E17D and P1D sections of lens from c.97_357del CRYBA1 mutant transgenic mice could not be distinguished from those of WT mice (Fig 3), with normal appearing anterior epithelia and bow regions and fiber cells exhibiting a normal developmental pattern and organization during early development of the lens and loss of nuclei in the differentiating central fiber cells by P1D. However, by 7 days after birth (P7D), lens sections from c.97_357del CRYBA1 mutant transgenic mice began to exhibit abnormalities in a few severely affected mice (figure 3G, H), including vacuolated equatorial epithelial cells associated with vacuolization and disorganization of the fiber cells beneath them. The severity of lens changes varied in different transgenic mice. The earliest posterior capsular rupture was detected was at P10D (Fig. 3I, J). Whether or not capsular rupture occurred, severe damage to the cortical and central fiber cells as well as the nuclei was seen by P12D with degenerating fiber cells detached from the anterior epithelia as well as many lacunae filled with proteinaceous debris (Fig. 3K, L). In addition, the anterior epithelial cells show increased vacuolization and loss of normal cuboidal morphology, especially in the central anterior area. By P16D, lens fiber cells showed increasing abnormalities including defective fiber cell elongation, migration, alignment, and denucleation distinctly different from that observed in WT lenses (Fig. 3M, N). The lens fiber cells were not properly oriented and showed structural abnormalities, including accumulation of degenerating cells in the posterior pole in which retained nuclei remained in all affected mice. Cataracts were eventually formed through a combination of disoriented and degenerating lens epithelial and fiber cells and posterior rupture of the, which was observed in most affected mice, although in a few mildly affected mice the changes were limited to accumulation of abnormal fiber cells and lacunae. In order to examine the specific effects on fiber cells more closely, wheat germ agglutinin was used to stain the cell membranes of the fiber cells (Fig. 3 O-W). Compared to the wt lens fiber cells (Fig. 3 O-Q), which show narrow gracile fiber cells extending across the lens, the fiber cells in c.97_357del CRYBA1 transgenic lenses are broader and distended, so that they are considerably wider than those in the control (seen best in Fig. 3 U-W). In addition, they are in some disarray, as some fiber cells are arranged vertically relative to the lens axis, so that they are cut in cross section and show an elongated hexagonal pattern (best seen in Fig. 3 R-T).

Quantitative RT-PCR of c.97_357del mutant CRYBA3 and β-crystallin mRNAs

Quantitative real-time PCR with normalization against GAPDH was performed to determine more accurately the expression level of the mutant CRYBA1 gene and its effect on expression of other crystallins. In mice transgenic for the minimal human CRYBB1 promoter, expression of the c.97_357del CRYBA1 mRNA increases through the embryonic and early postnatal stages of lens development. It attains its highest expression level at P7D at which time it is 16.8-fold higher than the endogenous mouse Cryba3/a1 mRNA, and then its expression decreases until by 5 weeks after birth its level is less than that of endogenous Cryba3/a1 (Fig. 4A). To investigate whether the decreased endogenous Cryba1 mRNA levels were the result of a feedback mechanism specific for this mRNA or whether they were due to a more general effect on the lens cells, the effects of p.Ile33_Ala119del βA3/A1 crystallin transgenic expression on additional genes in the β-crystallin family: Cryba2, Cryba4, Crybb1, Crybb2 and Crybb3, were examined. Quantitative RT-PCR revealed that all β-crystallin mRNAs are expressed at essentially normal levels as compared to WT through P7D, and then become significantly decreased in the c.97_357del CRYBA1 transgenic mouse lenses by P2W (figure 4B). At this time, Cryba1 Cryba2, Cryba4, Crybb1, Crybb2 and Crybb3 are decreased by 13.3, 7.0, 10.1, 6.3, 3.5, and 11.4-fold respectively. This is followed by a recovery of expression, giving a somewhat milder decrease relative to WT mouse lenses of approximately 5 fold at P3W, and slightly more than two fold at P5W and P8W. Toxicity of the p.Ile33_Ala119del βA3/A1 mutant crystallin with the accompanying overall decrease in synthesis of the endogenous crystallins implies a large overall decrease in protein synthesis. This resulted in a decrease in the mass of the p.Ile33_Ala119del βA3/A1 crystallin transgenic lens to 1.93 ± 0.23 mg from 8.85 ± 0.443 mg in the wild type and the accompanying decrease in the size of the lens as shown in Fig. 2B.

Clinically, no extralenticular effects were seen in the family segregating the c.215+1G>A mutant CRYBA1, nor were they seen in either the c.215+1G>A CRYBA1 or c.97_357del CRYBA1 transgenic mice (data not shown). In order to investigate the lens specific phenotype of this mutation further, extralenticular expression of transgenically expressed c. 97_357del CRYBA1 was examined and compared to that of endogenous Cryba1. The c. 97_357del CRYBA1 mRNA could be detected in lung, spleen, pancreas, intestine and testis at approximately tenfold lower levels than in the lens and in a number of other tissues at 100 to 1,000 fold lower levels, while endogenous Cryba1 mRNA was relatively lens specific with less than 1% of lens expression in the retina and testis only, and was not detectable in other tissues (figure 4C).

Transcript analysis in HLE cells

In order to investigate the mechanism of effects of the c.215+1G>A mutation on splicing of βA3/A1-crystallin expression further, HLE cells were transiently transfected with pcDNA4A/CRYBA1wt and pcDNA4A/ CRYBA1c.215+1G>A, in which the full length wt or c.215+1G>A mutant CRYBA1 gene was cloned into the pcDNA4A plasmid between the Kpn1 and Xhol sites. This vector uses the cmv promoter driving the full length wt or c. 215+1G>A mutant CRYBA1 gene with N-his and Xpress tags. RT-PCR products from cells transfected with pcDNA4A/CRYBA1wt showed a band at 572bp, the expected size. In contrast, RT-PCR of pcDNA4A/ CRYBA1c.215+1G>A transfected cells yielded products

around 300bp, the size predicted for an mRNA skipping exons 3 and 4 (Fig. 5A, B). Sequencing of both bands confirmed that the c.215+1G>A mutant underwent altered splicing in which exons 3 and 4 were skipped (figure 5A), similar to that seen in mice transgenic for the c.215+1G>A mutant and WT genomic sequences. In addition to the major bands, both the wt and c.215+1G>A mutant transfected cells showed several minor bands after RT-PCR. When these were cloned and sequenced, the WT transfected cells included two more transcripts, one of 430 bp in which exon 4 was skipped and another of 246bp in which exons 2, 3 and 4 were skipped. The c.215+1G>A mutant transfected cells showed 3 additional transcripts, in one of which exon 3 was skipped, in a second of which exons 2 and 3 were skipped, and in the third of which exons 2, 3, and 4 were skipped (data not shown). Among all the transcripts, only the full length transcript seen in the WT and the transcript in which exons 3 and 4 were skipped in the c.215+1G>A mutant maintained the translation frame. All other transcripts were predicted to produce premature terminations before the final exon. Western blotting confirmed that only the full length transcript in WT cells and the c.215+1G>A mutant in which exons 3 and 4 were skipped were translated into proteins (Fig. 5C).

Splicing in which two or more exons are skipped is usually seen in low-abundance mRNA species and is often associated with alternative splicing, neither of which is the case for CRYBA1. Thus, the possibility that the favored splice product for the c.215+1G>A mutant transcript might actually be one in which a single exon was skipped but which was subject to nonsense mediated decay seemed likely. The low level of messages in which frameshift changes were predicted to result in premature termination was also consistent with Nonsense-Mediated Decay. In order to investigate this possible mechanism further, transfected HLE cells were treated with PTC124 for 48 hours in order to inhibit nonsense mediated decay. The resulting RT-PCR showed no extra transcripts, and no significant shifts in the densities of bands representing the various transcripts generated either by the wild type or c.215+1G>A mutant gene with increasing amounts of PTC124 (Fig. 5B). This strongly suggests that the transcript lacking exons 3 and 4 is naturally favored by intrinsic splicing order preferences and escapes nonsense mediated decay on that basis.

Cellular Mechanism of p.Ile33_Ala119del CRYBA3 mutant Toxicity

In order to elucidate the mechanism through which expression of the p.Ile33_Ala119del CRYBA3 mutant protein is toxic to lens epithelia and especially to fiber cells, expression of sentinel proteins marking the unfolded protein response (UPR) was examined. RT-PCR analysis of mouse lenses transgenic for the c.97_357del CRYBA3 mRNA showed that transcription of unfolded protein responsive genes including BiP/GRP78 (HSPA5 in humans) and CHOP (DDIT3 in humans) was increased (Figure 6). The timing of this increase generally followed expression of the c.97_357del CRYBA1 mutant and correlated with decreases in expression of endogenous crystallins and the histological changes seen in the lens. Both Chop and Grp78 began rising at about P1D, increasing 3 fold by P7D and 7-13-fold by P2W, and then slowly decreasing thereafter (Fig. 6A). In addition, while careful examination shows some spliced Xbp1 (X-box binding protein 1) in lenses from c. 97_357del CRYBA3 mutant transgenic mice at ages greater than P7D, the highest level of

Xbp1(S) was detected at P7D when mutant CRYBA3/A1 expression also showed peak expression (figure 6B).

Because expression of marker proteins for the unfolded protein response (UPR) peaked at P2W, we performed RT^2 Profiler PCR Array focusing on the mouse UPR at P7D and P14D. Expression of genes in the UPR and apoptotic pathways between the c.97_357del and WT CRYBA1 showed little difference in P7D lenses, but at P2W over half the genes tested showed over a 2-fold increase (figure 6C). While increases in all pathways leading to the UPR and apoptosis suggest that these pathways are widely activated, some parts of the pathway appear to be particularly subject to activation in this cataract (figure S1). These include genes encoding proteins carrying out unfolded protein binding, of which 9 of 21 candidates tested were elevated 2 fold or more, and ER associated degradation (ERAD), of which 10 of 19 candidates tested were elevated, 3 greater than 5 fold. Another group of genes whose expression was dramatically increased was transcription factors, of which 7 of 17 candidates tested were elevated, 3 greater than 5 fold. The mRNA levels for pathways including heat shock proteins, effectors of apoptosis, proteins regulating translation, and ubiquitination were somewhat more moderately elevated, including 3 of 10, 5 of 18, 1 of 4, and 3 of 13 members respectively. In contrast, less than 20% of the candidates in the ER protein folding quality control, cholesterol metabolism regulation, protein folding, and disulfide isomerization pathways were increased.

Increased mRNA levels for over half of the genes in these pathways by over 2-fold in P2W c.97_357del CRYBA1 mice compared with WT CRYBA1 mice (Figure S1), provides strong evidence that the c.97_357del CRYBA1 mRNA is translated into the p.Ile33_Ala119del CRYBA3 protein and activates the UPR and then the apoptotic apparatus in the lens. To confirm that the UPR actually induces apoptosis in the p.Ile33_Ala119del CRYBA3 transgenic lenses, terminal deoxynucleotidyl transferase dUTP nick end labeling (TUNEL) assay was performed. As seen in Figure 7, TUNEL staining of p.Ile33_Ala119del CRYBA3 and WT transgenic lenses demonstrates that karyolysis was inhibited resulting in nuclear fragments in the posterior pole of c.97_357del mutant but not WT CRYBA1 mice lens by 10 days after birth. However, no TUNEL positive cells are seen in the cortical bow regions of lenses of either line of transgenic mice (Fig. 7). In addition, there is distinctly more nuclear material in the posterior pole of the c.97_357del cDNA mutant lenses.

In order to further investigate the molecular events leading to induction of the UPR and apoptotic pathways, subcellular localization of the p.Ile33_Ala119del CRYBA3 protein was investigated and contrasted to that of the wt CRYBA3 protein in cultured HLE cells (Fig. S2). The wt βA3/A1-crystallin protein can be seen to be diffusely spread throughout the cytoplasm, with little colocalization with the ER (Fig. S2A). In contrast, the p.Ile33_Ala119del βA3/A1-crystallin is seen primarily in aggregates, of which a subset seem to colocalize with the ER, while the remainder do not. The ER in areas of colocalization appears to be thickened, with some areas showing larger globular shapes. Colocalization of wt and p.Ile33_Ala119del βA3/A1-crystallin was also examined (Fig. S2B). In cells transfected with the wt βA3/A1-crystallin staining for both βA3/A1-crystallin and α-crystallin is diffuse, with some areas of overlap, but most of both proteins independently distributed. In contrast, cells transfected with the p.Ile33_Ala119del βA3/A1-crystallin show

large aggregates superimposed on this background, and these appear to contain both βA3/A1- andα-crystallin. This is seen most clearly when expression of the p.Ile33_Ala119del βA3/A1-crystallin is relatively low (Fig. S2B, middle row). When expression of the p.Ile33_Ala119del βA3/A1-crystallin increases, additional aggregates appear, only some of which colocalize with α-crystallin.

To characterize possible differential degradation of the WT and p.Ile33_Ala119del mutant βA3/A1 proteins further, pcDNA3.1/CRYBA1-cDNA and pcDNA3.1/ CRYBA1 c. 97_357del cDNA were transiently transfected into HLE cells and immunofluorescence staining was examined by confocal fluorescence microscopy (Fig. S3). Cells were transfected using cmv promoter driven constructs for the WT and p.Ile33_Ala119del mutant βA3/A1-crystallins proteins. Confocal micrographs of cells transfected with lower levels of βA3/A1-crystallin demonstrated aggregation of c.97_357del mutant but not WT βA3/A1-crystallin protein in the cytosol of transfected cells (Fig. S3A and C). However, at this lower level of expression, neither mutant nor WT proteins colocalized with lysosomes as indicated by colocalization neither with LysoTracker nor p62 (also named sequestosome 1, SQSTM1), a scaffolding protein implicated in apoptosis and ubiquitin-mediated autophagy that is a common component of protein aggregates. However, cells expressing higher levels of βA3/A1-crystallin (Fig. S3B and D) showed larger and denser clumps of βA3/A1-crystallin protein as well as some localized higher concentrations of the WT protein, although this continued to show a diffuse pattern similar to that seen at lower concentrations. In contrast to the results seen with lower expression constructs, at higher protein levels some but not all of the granules of the mutant protein colocalized with lysotracker. In addition, the pattern of p62 staining shifted from the generally diffuse pattern seen in the WT cells to a granular pattern overlapping granules of the p.Ile33_Ala119del mutant βA3/A1-crystallins protein. When combined with the α-crystallin localization data, these suggest that at low expression levels the mutant βA3/A1 crystallin is bound by α-crystallin while at higher concentrations the denatured mutant protein exceeds the α-crystallin binding capacity and either is recognized by p62, which then mediates its entry into lysosomes to form autophagosomes or precipitates into large aggregates within the cell.

To further check for binding of the p.Ile33_Ala119del mutant βA3/A1-crystallin to α-crystallin, soluble proteins were extracted from lenses of P7D c.97_357del mutant CRYBA3 mice and analyzed by size exclusion chromatography on a SEC650 column (Fig. S4). The lens crystallins eluted in a typical three peak (α-, β-, γ-crystallin) profile with large aggregated proteins eluting at the exclusion volume. The p.Ile33_Ala119del mutant βA3/A1-crystallin protein eluted to some extent in the large aggregates, but primarily with the α-crystallin peak. The endogenous βA3/A1-crystallin protein eluted primarily in the β-crystallin peak, slightly behind the α-crystallin peak containing the p.Ile33_Ala119del mutant βA3/A1-crystallin protein. This suggests that most of the p.Ile33_Ala119del mutant βA3/A1-crystallin is found either bound to α-crystallin or in the insoluble fraction of the lens protein.

Discussion

This study delineates the cellular mechanism of cataractogenesis of the CRYBA1 c. 215+1G>A mutation previously identified as a cause of autosomal dominant cataracts in a large Indian family (Kannabiran et al. 1998; Scott et al. 1994). The CRYBA1 c.215+1G>A splice mutant avoids nonsense mediated decay by preferentially skipping exons 3 and 4, returning in-frame to exons 5 and 6 to produce a c.97_357del CRYBA1 mRNA. This results in expression of a 15 kDa p.Ile33_Ala119del mutant βA3-crystallin that is unstable and toxic to the developing lens fiber cells, activating the UPR and apoptosis beginning around 7 days after birth and peaking at 14 days when expression of Chop and Grp78 are increased and spliced XBP1 is detected. Results of the UPR, apoptosis, and perhaps direct toxicity of the 15 kDa p.Ile33_Ala119del mutant βA3-crystallin on lens cells are seen histologically in mice transgenic for c.97_357del CRYBA1 cDNA as vacuolization and degeneration of the lens fiber cells accompanied by a smaller spherical lens, opacity, and rupture of the posterior lens capsule, all found in cataract formation.

Mutations in crystallins or other lens proteins sufficient in and of themselves to denature the target and cause protein aggregation usually damage lens cells directly and result in congenital cataract, while if they merely destabilize the protein, increasing susceptibility to environmental insults, tend be bound by α-crystallin, eventually forming high molecular weight aggregates that scatter light and contribute to age-related cataract (Shiels and Hejtmancik 2007). In this regard, expression of a mutant crystallin with a damaging effect on the lens potentially could pose a serious challenge to lens cell homeostasis. This risk is compounded because lens fiber cells, in which β-crystallin expression is highest (Hawse et al. 2005), have the capacity neither to synthesize new proteins nor to degrade and turn over large amounts of damaged or denatured proteins. Modeling the effects of the mutant βA3-crystallin required a high level of expression not provided by the chicken CRYAA basic promoter used for our initial studies determining the splicing abnormalities caused by the CRYBA1 c.215+1G>A mutation, but was possible using a CRYBB1 driven minigene, known to provide higher protein expression levels (Chen et al. 2001). While the mRNA levels resulting from this construct were significantly above those of the endogenous crystallins at some stages of development, expression at the protein level was still somewhat below that of the endogenous βA3-crystallin (Figs. 2 and 4). Even this higher level of expression was not capable of inducing the unfolded protein response (UPR) in cultured lens cells, which as dividing cells maintain their protein synthetic and degrading capabilities as opposed to the lens, the cells of which are terminally differentiated with no further cell division and reduced capacity for protein degradation.

One initial question in this investigation was the mechanism through which the c.97_357del CRYBA1 mutant mRNA escaped nonsense mediated decay, a process through which cells are protected from the toxic effects of mutant proteins through degradation of mRNAs with premature termination occurring more than about 50 bases before the final exon of the encoding gene (Chang et al. 2007). On the basis of the genomic data shown in Fig. 1 it initially seemed likely that most of the c.215+1G>A mutant HnRNA would skip only exon 4 and would be subject to nonsense mediated decay, perhaps with a small amount of the mutant mRNA being alternatively spliced by skipping 2 exons and producing a

correspondingly small amount of toxic mutant protein, as has been described for human coagulation factor VII (Ding et al. 2005). However, this was not consistent with the splicing data shown in Fig. 5. The presence of the c.97_357del CRYBA3 mutant mRNA in the control samples and the lack of a second mRNA product skipping a single exon in the presence of PTC124, which inhibits nonsense mediated decay, strongly suggests that the c. 97_357 del CRYBA1 mRNA is the predominant product of the CRYBA1 c.215+1G>A mutant gene. While mRNA splicing is a complicated process (Black 2003) and it is possible that there might be tissue specific or other effects not seen in the tissue culture system used here, similar results have been seen previously in other genes. Introns are spliced out in a preferred but not necessarily sequential order (Kessler et al. 1993), and this can result in complex effects on splice products resulting from a single splice mutation (Schwarze et al. 1999). It is likely that intron 3 of the CRYBA1 mRNA is removed before intron 2, resulting in skipping of both exons 3 and 4 in the c.215+1G>A mutant mRNA, similar to the splicing mutations previously reported for *COL5A1* (Takahara et al. 2002) and *OXCT1* (Hori et al. 2013).

The resulting p.Ile33_Ala119del mutant βA3/A1-crystallin protein is unstable when compared to the native protein. This is consistent with the known structure of the βγ-crystallins, which comprises a two-domain, four Greek-key motif protein fold (Blundell et al. 1981; Slingsby and Clout 1999). The p.Ile33_Ala119del mutant βA3/A1-crystallin protein would be missing the first and second Greek key motifs, which form the N domain. However the β-crystallins have extended inter-domain interactions, and motifs 3 and 4 of the βA3-crystallin N and C domains are aligned in an antiparallel fashion with each other. Thus, deletion of the amino terminal domain would be predicted to result in an isolated carboxyl terminal domain with greatly decreased stability (Mayr et al. 1997; Wenk et al. 2000). Such an unstable protein product would be subject to denaturation and might potentially stimulate the unfolded protein response (UPR). Interestingly, while lens crystallins are soluble cytosolic proteins, they are synthesized on a combination of free, microfilament-attached, and rough endoplasmic reticulum associated ribosomes in approximately equal proportions (Ramaekers et al. 1983), suggesting that an unstable crystallin might be expected to induce the UPR. Conversely, identification of the p.Ile33_Ala119del mutant βA3/A1-crystallin protein in the soluble fraction of lens extracts and its normal distribution in the lens cytoplasm of cultured lens cells suggests that at least a sizeable fraction of the mutant protein is soluble and somewhat stable for at least a short duration, although by 6 months of age most of the p.Ile33_Ala119del βA3/A1-crystallin is degraded into a 10kDa fragment that is found largely in the insoluble fraction of lens extracts.

The UPR comprises a set of evolutionarily conserved cell signaling pathways that combat endoplasmic reticulum stress (ER stress) caused by increased levels of unfolded or misfolded proteins within the ER lumen by upregulating endoplasmic reticulum associated degradation (ERAD) proteins and chaperones (Sovolyova et al. 2014). When the UPR fails to achieve ER homeostasis it can also induce apoptosis(Lai et al. 2007; Rasheva and Domingos 2009), largely through the intrinsic or mitochondrial-mediated pathway (Gupta et al. 2010; Szegezdi et al. 2008) but also through PERK dependent genetic regulation. This includes repression of microRNAs (Gupta et al. 2012), ATF6 activation of transcription including synthesis of XBP1, and IRE1 mediated cleavage of XBP1, which induces

transcription of a variety of mediators including P58 (Gorman et al. 2012). The molecular chaperone immunoglobin-binding protein (BiP, also called HSPA5, MLF2, or GRP78) is a sentinel marker for the UPR. It maintains major sensors (IRE1, ATF6, and PERK) in an inactive state. Upon accumulation of unfolded proteins BiP dissociates from the sensors, which leads to their activation and triggering of the UPR. In addition, full length XBP1 requires the endoribonuclease domain of active IRE1 for processing into active (spliced) sXBP1. Splicing of XBP1 is a key marker for IRE1 activation by BiP dissociation. Chop (also called DDIT3) is a transcription factor that inhibits activation of a number of genes when activated by ER stress to promote apoptosis.

Previously, support for the role of the UPR in cataractogenesis has been mixed and is sometimes confined to the metabolically more active lens epithelial cells. However, evidence supporting its potential role is increasing. The UPR has been suggested to contribute to a number of types of cataract including selenite cataracts in rats (Palsamy et al. 2014), and cultured lens epithelial cells from galactosemic rats (Mulhern et al. 2006). Expression of two abnormal collagens in transgenic mice has been shown to activate the UPR and induce cataracts, but only one of the abnormal collagens caused cell death (Firtina et al. 2009). Finally, transgenic expression of mutant CRYAA and GJA8 in mice has been shown to activate parts of the UPR (Alapure et al. 2012; Andley and Goldman 2015), although because of the relatively modest extent of this activation in GJA8 mutant mice the authors suggested that it was unlikely to be a major factor in the pathogenesis of the cataract. That the UPR is activated by the p.Ile33_Ala119del mutant βA3/A1-crystallin protein is indicated both by increases in Grp78 and Chop, peaking at P2W and coinciding with the maximal effects on crystallin expression, and the presence of spliced XBP1 most obvious at the same time but continuing through P8W. The increase in these key regulators of the UPR as well as increases of the mRNA levels of many components of the various UPR implicate the UPR causally in the c.215+1G>A CRYBA1 cataracts. However, while the histology of the mutant lenses certainly indicates cell death accompanies activation of the UPR, this was not seen in cell culture, probably because of the relatively lower expression of the p.Ile33_Ala119del mutant βA3-crystallin protein and dilution or turnover of the toxic protein in the dividing cells as opposed to the terminally differentiated cells in the lens.

One interesting question that is beyond the scope of the present work is how the UPR induced inhibition of protein synthesis and eventual initiation of apoptosis interact with the ongoing fiber cell elongation and loss of organelles, especially nuclei, that are a part of normal lens development at this stage. One interesting possibility consistent with the persistence of TUNEL positive nuclear fragments seen in figure 7 is that they both might contribute to impairment of the posterior lens structures that eventually results in posterior rupture of the lens nucleus. TUNEL positive degenerating nuclei are normal earlier in lens development (Wride and Sanders 1998), but are not normally present at this age. Fiber cells of the lens nucleus are fully differentiated and should not undergo apoptosis, so these TUNEL positive cells presumably represent incomplete karyolysis during fiber cell development. Nuclear persistence does occur in a number of other cataract models (Cammarata et al. 1999; Capetanaki et al. 1989; Chung et al. 2007; Dunia et al. 1990; Perez-Castro et al. 1993). Supporting this possibility, inhibition of activity of Ncoa6, a coactivator of a number of nuclear receptors and transcription factors, in transgenic mice has been

shown to result in a similar histological phenotype also accompanied by inhibition of nucleolysis and induction of TUNEL positive fragments, presumably by inducing a prolonged but incomplete apoptosis-like process (Wang et al. 2010). The histological phenotype of the p.Ile33_Ala119del βA3-crystallin mutant also appears similar to that of the previously described c.119_123dup CRYGC mutation (Ma et al. 2011). Both cataracts result from expression of an unstable crystallin that is probably toxic to elongating lens fiber cells, although activation of the UPR and apoptosis pathways was not characterized in the latter as it was for the present mutation.

In addition to the toxic effect on lens cells, the CRYBA1 c.215+1G>A mutation might conceivably be expected to have a number of extralenticular effects. It has been reported that the Nuc1 mutation, a 27 base pair insertion in exon 6 of the βA3/A1-crystallin gene on rat chromosome 10, results in abnormalities of both the lens and the retinal neurons and vessels (Sinha et al. 2008). However, no retinal signs or symptoms were reported in the Pakistani family in which the CRYBA1 c.215+1G>A mutation cataracts occurred, and no retinal abnormalities were observed in our mouse models. Although the −432/+30 fragment of the chicken βB1-crystallin promoter we used to drive high level transgene expression to lens fiber cells is relatively lens specific, its retinal expression is still greater than the wild type CRYBA1 gene (Fig. 4 and reference (Chen et al. 2001)). However, while we did not observe any retinal abnormalities in either humans or mice with this mutation we were unable to carry out retinal functional studies or more precise histological characterization of any possible retinal changes.

In summary, these results provide *in vivo* evidence of a role for the UPR in cataract formation in response to accumulation of the p.Ile33_Ala119del mutant CRYBA3/A1 protein. However, while it seems likely that induction of the UPR is an integral part of cataractogenesis seen with this mutation, there is no formal proof that the appearance of UPR is sufficient to lead to the severe cataracts seen here. Severe lens phenotypes can occur without an initial activation of the UPR, and the UPR conceivably could be a consequence of the subsequent lens phenotype rather than its cause. The underlying molecular mechanism for the autosomal dominant zonular cataracts with sutural opacities in this Indian family begins with the CRYBA1 c.215+1G>A mutant mRNA escaping nonsense mediated decay by skipping both exons 3 and 4. This results in an in-frame deletion and synthesis of a p.Ile33_Ala119del mutant protein causing toxicity and abnormal maturation and degeneration of differentiating lens fibers leading to a small spherical lens, cataract, and lens capsular rupture. On a cellular level, the mutant lenses accumulated p.Ile33_Ala119del mutant βA3/1-crystallin causing activation of the UPR stress signaling pathway and inhibition of normal protein synthesis, and ending in a modified apoptosis of the lens fiber cells. It seems likely that, as opposed to age-related cataracts that tend to involve slow denaturation of crystallins and binding by α-crystallin chaperones (Datiles et al. 2008), this is a common mechanism for early onset congenital cataracts resulting from destabilizing mutations in crystallins or other highly expressed lens proteins.

Supplementary Material

Refer to Web version on PubMed Central for supplementary material.

Acknowledgements

This work was supported by the National Eye Institute: EY000281.

References

Alapure BV, Stull JK, Firtina Z, Duncan MK. The unfolded protein response is activated in connexin 50 mutant mouse lenses. Exp Eye Res. 2012; 102:28–37. doi: 10.1016/j.exer.2012.06.004. [PubMed: 22713599]

Andley UP, Goldman JW. Autophagy and UPR in alpha-crystallin mutant knock-in mouse models of hereditary cataracts. Biochim Biophys Acta. 2015 doi: 10.1016/j.bbagen.2015.06.001.

Basti S, Hejtmancik JF, Padma T, Ayyagari R, Kaiser-Kupfer MI, Murty JS, Rao GN. Autosomal dominant zonular cataract with sutural opacities in a four-generation family. American Journal of Ophthalmology. 1996; 121:162–168. [PubMed: 8623885]

Bateman JB, Geyer DD, Flodman P, Johannes M, Sikela J, Walter N, Moreira AT, Clancy K, Spence MA. A new betaA1-crystallin splice junction mutation in autosomal dominant cataract. Invest Ophthalmol.Vis.Sci. 2000; 41:3278–3285. [PubMed: 11006214]

Black DL. Mechanisms of alternative pre-messenger RNA splicing. Annu Rev Biochem. 2003; 72:291–336. doi: 10.1146/annurev.biochem.72.121801.161720 121801.161720 [pii]. [PubMed: 12626338]

Blundell T, Lindley P, Miller L, Moss D, Slingsby C, Tickle I, Turnell B, Wistow G. The molecular structure and stability of the eye lens: x-ray analysis of gamma-crystallin II. Nature. 1981; 289:771–777. [PubMed: 7464942]

Burdon KP, Wirth MG, Mackey DA, Russell-Eggitt IM, Craig JE, Elder JE, Dickinson JL, Sale MM. Investigation of crystallin genes in familial cataract, and report of two disease associated mutations. Br.J.Ophthalmol. 2004; 88:79–83. [PubMed: 14693780]

Cammarata PR, Zhou C, Chen G, Singh I, Reeves RE, Kuszak JR, Robinson ML. A transgenic animal model of osmotic cataract. Part 1: over-expression of bovine Na+/myo-inositol cotransporter in lens fibers. Invest Ophthalmol.Vis.Sci. 1999; 40:1727–1737. [PubMed: 10393042]

Capetanaki Y, Smith S, Heath JP. Overexpression of the vimentin gene in transgenic mice inhibits normal lens cell differentiation. Journal of Cell Biology. 1989; 109:1653–1664. [PubMed: 2793935]

Chang YF, Imam JS, Wilkinson MF. The nonsense-mediated decay RNA surveillance pathway. Annu Rev Biochem. 2007; 76:51–74. doi: 10.1146/annurev.biochem.76.050106.093909. [PubMed: 17352659]

Chen WV, Hejtmancik JF, Piatigorsky J, Duncan MK. The mouse betaB1-crystallin promoter: strict regulation of lens fiber cell specificity. Biochimica et Biophysica Acta. 2001; 1519:30–38. [PubMed: 11406268]

Chepelinsky AB, King CR, Zelenka PS, Piatigorsky J. Lens-specific expression of the chloramphenicol acetyltransferase gene promoted by 5′ flanking sequences of the murine alpha A-crystallin gene in explanted chicken lens epithelia. Proceedings of the National Acadamy of Sciences USA. 1985; 82:2334–2338.

Chung J, Berthoud VM, Novak L, Zoltoski R, Heilbrunn B, Minogue PJ, Liu X, Ebihara L, Kuszak J, Beyer EC. Transgenic overexpression of connexin50 induces cataracts. Exp Eye Res. 2007; 84:513–28. doi: S0014-4835(06)00446-5 [pii] 10.1016/j.exer.2006.11.004. [PubMed: 17217947]

Cohen D, Bar-Yosef U, Levy J, Gradstein L, Belfair N, Ofir R, Joshua S, Lifshitz T, Carmi R, Birk OS. Homozygous CRYBB1 deletion mutation underlies autosomal recessive congenital cataract. Invest Ophthalmol.Vis.Sci. 2007; 48:2208–2213. [PubMed: 17460281]

Datiles MB III, Ansari RR, Suh KI, Vitale S, Reed GF, Zigler JS Jr. Ferris FL III. Clinical detection of precataractous lens protein changes using dynamic light scattering. Archives of Ophthalmology. 2008; 126:1687–1693. [PubMed: 19064850]

Devi RR, Yao W, Vijayalakshmi P, Sergeev YV, Sundaresan P, Hejtmancik JF. Crystallin gene mutations in Indian families with inherited pediatric cataract. Molecular Vison. 2008; 14:1157–1170.

Ding Q, Wu W, Fu Q, Wang X, Hu Y, Wang H, Wang Z. Novel aberrant splicings caused by a splice site mutation (IVS1a+5g>a) in F7 gene. Thromb Haemost. 2005; 93:1077–81. doi: 05061077 [pii] 10.1267/THRO05061077. [PubMed: 15968391]

Dunia I, Pieper F, Manenti S, van dK, Devilliers G, Benedetti EL, Bloemendal H. Plasma membrane-cytoskeleton damage in eye lenses of transgenic mice expressing desmin. Eur.J.Cell Biol. 1990; 53:59–74. [PubMed: 2076709]

Firtina Z, Danysh BP, Bai X, Gould DB, Kobayashi T, Duncan MK. Abnormal expression of collagen IV in lens activates unfolded protein response resulting in cataract. J Biol Chem. 2009; 284:35872–84. doi: 10.1074/jbc.M109.060384. [PubMed: 19858219]

Gorman AM, Healy SJ, Jager R, Samali A. Stress management at the ER: regulators of ER stress-induced apoptosis. Pharmacol Ther. 2012; 134:306–16. doi: 10.1016/j.pharmthera.2012.02.003. [PubMed: 22387231]

Gu Z, Ji B, Wan C, He G, Zhang J, Zhang M, Feng G, He L, Gao L. A splice site mutation in CRYBA1/A3 causing autosomal dominant posterior polar cataract in a Chinese pedigree. Molecular Vison. 2010; 16:154–160.

Gupta S, Cuffe L, Szegezdi E, Logue SE, Neary C, Healy S, Samali A. Mechanisms of ER Stress-Mediated Mitochondrial Membrane Permeabilization. Int J Cell Biol. 20102010:170215. doi: 10.1155/2010/170215. [PubMed: 20169117]

Gupta S, Read DE, Deepti A, Cawley K, Gupta A, Oommen D, Verfaillie T, Matus S, Smith MA, Mott JL, Agostinis P, Hetz C, Samali A. Perk-dependent repression of miR-106b-25 cluster is required for ER stress-induced apoptosis. Cell Death Dis. 2012; 3:e333. doi: 10.1038/cddis.2012.74 cddis201274 [pii]. [PubMed: 22739985]

Hawse JR, DeAmicis-Tress C, Cowell TL, Kantorow M. Identification of global gene expression differences between human lens epithelial and cortical fiber cells reveals specific genes and their associated pathways important for specialized lens cell functions. Mol Vis. 2005; 11:274–83. doi: v11/a32 [pii]. [PubMed: 15851978]

Hejtmancik, JF.; Kaiser-Kupfer, MI.; Piatigorsky, J. Molecular biology and inherited disorders of the eye lens. In: Scriver, CR.; Beaudet, AL.; Valle, D.; Sly, WS.; Childs, B.; Kinzler, KW.; Vogelstein, B., editors. The Metabolic and Molecular Basis of Inherited Disease. Vol. 8. McGraw Hill; New York: 2001. p. 6033-6062.

Hope JN, Chen HC, Hejtmancik JF. BetaA3/A1-crystallin association: role of the amino terminal arm. Protein Engineering. 1994; 7:445–451. [PubMed: 8177894]

Hori T, Fukao T, Murase K, Sakaguchi N, Harding CO, Kondo N. Molecular basis of two-exon skipping (exons 12 and 13) by c.1248+5g>a in OXCT1 gene: study on intermediates of OXCT1 transcripts in fibroblasts. Hum Mutat. 2013; 34:473–80. doi: 10.1002/humu.22258. [PubMed: 23281106]

Jobby MK, Sharma Y. Calcium-binding to lens betaB2- and betaA3-crystallins suggests that all beta-crystallins are calcium-binding proteins. FEBS J. 2007; 274:4135–4147. [PubMed: 17651443]

Kannabiran C, Rogan PK, Olmos L, Basti S, Rao GN, Kaiser-Kupfer M, Hejtmancik JF. Autosomal dominant zonular cataract with sutural opacities is associated with a splice site mutation in the betaA3/A1-crystallin gene. Molecular Vision. 1998; 4:21–26. [PubMed: 9788845]

Kessler O, Jiang Y, Chasin LA. Order of intron removal during splicing of endogenous adenine phosphoribosyltransferase and dihydrofolate reductase pre-mRNA. Mol Cell Biol. 1993; 13:6211–22. [PubMed: 8413221]

Khan AO, Aldahmesh MA, Meyer B. Recessive Congenital Total Cataract with Microcornea and Heterozygote Carrier Signs Caused by a Novel Missense CRYAA Mutation (R54C). Am.J.Ophthalmol. 2007

Lai E, Teodoro T, Volchuk A. Endoplasmic reticulum stress: signaling the unfolded protein response. Physiology (Bethesda). 2007; 22:193–201. doi: 10.1152/physiol.00050.2006. [PubMed: 17557940]

Ma Z, Yao W, Theendakara V, Chan CC, Wawrousek E, Hejtmancik JF. Overexpression of human {gamma}C-crystallin 5bp duplication Disrupts Lens Morphology in Transgenic Mice. Invest Ophthalmol Vis.Sci. 2011

Mayr EM, Jaenicke R, Glockshuber R. The domains in gammaB-crystallin: identical fold-different stabilities. J Mol Biol. 1997; 269:260–9. doi: S0022-2836(97)91033-0 [pii] 10.1006/jmbi.1997.1033. [PubMed: 9191069]

Meyer E, Rahman F, Owens J, Pasha S, Morgan NV, Trembath RC, Stone EM, Moore AT, Maher ER. Initiation codon mutation in betaB1-crystallin (CRYBB1) associated with autosomal recessive nuclear pulverulent cataract. Molecular Vison. 2009; 15:1014–1019.

Mulhern ML, Madson CJ, Danford A, Ikesugi K, Kador PF, Shinohara T. The unfolded protein response in lens epithelial cells from galactosemic rat lenses. Invest Ophthalmol Vis Sci. 2006; 47:3951–9. doi: 10.1167/iovs.06-0193. [PubMed: 16936110]

Palsamy P, Bidasee KR, Shinohara T. Selenite cataracts: activation of endoplasmic reticulum stress and loss of Nrf2/Keap1-dependent stress protection. Biochim Biophys Acta. 2014; 1842:1794–805. doi: 10.1016/j.bbadis.2014.06.028. [PubMed: 24997453]

Perez-Castro AV, Tran VT, Nguyen-Huu MC. Defective lens fiber differentiation and pancreatic tumorigenesis caused by ectopic expression of the cellular retinoic acid-binding protein I. Development. 1993; 119:363–375. [PubMed: 8287793]

Pras E, Frydman M, Levy-Nissenbaum E, Bakhan T, Raz J, Assia EI, Goldman B. A nonsense mutation (W9X) in CRYAA causes autosomal recessive cataract in an inbred Jewish Persian family. Invest Ophthalmol.Vis.Sci. 2000; 41:3511–3515. [PubMed: 11006246]

Ramaekers FC, Benedetti EL, Dunia I, Vorstenbosch P, Bloemendal H. Polyribosomes associated with microfilaments in cultured lens cells. Biochim Biophys Acta. 1983; 740:441–8. [PubMed: 6309238]

Rasheva VI, Domingos PM. Cellular responses to endoplasmic reticulum stress and apoptosis. Apoptosis. 2009; 14:996–1007. doi: 10.1007/s10495-009-0341-y. [PubMed: 19360473]

Riazuddin SA, Yasmeen A, Yao W, Sergeev YV, Zhang Q, Zulfiqar F, Riaz A, Riazuddin S, Hejtmancik JF. Mutations in βB3-Crystallin Associated with Autosomal Recessive Cataract in Two Pakistani Families. Invest Ophthalmol.Vis.Sci. 2005; 46:2100–2106. [PubMed: 15914629]

Safieh LA, Khan AO, Alkuraya FS. Identification of a novel CRYAB mutation associated with autosomal recessive juvenile cataract in a Saudi family. Molecular Vison. 2009; 15:980–984.

Schwarze U, Starman BJ, Byers PH. Redefinition of exon 7 in the COL1A1 gene of type I collagen by an intron 8 splice-donor-site mutation in a form of osteogenesis imperfecta: influence of intron splice order on outcome of splice-site mutation. Am J Hum Genet. 1999; 65:336–44. doi: S0002-9297(07)62050-3 [pii] 10.1086/302512. [PubMed: 10417276]

Scott MH, Hejtmancik JF, Wozencraft LA, Reuter LM, Parks MM, Kaiser-Kupfer MI. Autosomal dominant congenital cataract: Interocular phenotypic heterogeneity. Ophthalmology. 1994; 101:866–871. [PubMed: 8190472]

Shiels A, Bennett TM, Hejtmancik JF. Cat-Map: putting cataract on the map. Molecular Vison. 2010; 16:2007–2015.

Shiels A, Hejtmancik JF. Genetic origins of cataract. Archives of Ophthalmology. 2007; 125:165–173. [PubMed: 17296892]

Sinha D, Klise A, Sergeev Y, Hose S, Bhutto IA, Hackler L Jr. Malpic-Llanos T, Samtani S, Grebe R, Goldberg MF, Hejtmancik JF, Nath A, Zack DJ, Fariss RN, McLeod DS, Sundin O, Broman KW, Lutty GA, Zigler JS Jr. betaA3/A1-crystallin in astroglial cells regulates retinal vascular remodeling during development. Mol.Cell Neurosci. 2008; 37:85–95. [PubMed: 17931883]

Slingsby C, Clout NJ. Structure of the crystallins. Eye. 1999; 13:395–402. [PubMed: 10627816]

Sovolyova N, Healy S, Samali A, Logue SE. Stressed to death - mechanisms of ER stress-induced cell death. Biol Chem. 2014; 395:1–13. doi: 10.1515/hsz-2013-0174/j/hsz.2014.395.issue-1/hsz-2013-0174/hsz-2013-0174.xml [pii] /j/bchm.just-accepted/hsz-2013-0174/hsz-2013-0174.xml [pii]. [PubMed: 24002662]

Srivastava OP, Srivastava SK. Purification and characterization of a socium deoxycholate- activatable proteinase activity, possibly associated with betaA3/A1-crystallin from human lenses. Investigative Ophthalmology and Visual Science. 1996; 37:1949–1949.

Sun W, Xiao X, Li S, Guo X, Zhang Q. Mutation analysis of 12 genes in Chinese families with congenital cataracts. Mol Vis. 2011; 17:2197–206. doi: 238 [pii]. [PubMed: 21866213]

Szegezdi E, Herbert KR, Kavanagh ET, Samali A, Gorman AM. Nerve growth factor blocks thapsigargin-induced apoptosis at the level of the mitochondrion via regulation of Bim. J Cell Mol Med. 2008; 12:2482–96. doi: 10.1111/j.1582-4934.2008.00268.x JCMM268 [pii]. [PubMed: 18266951]

Takahara K, Schwarze U, Imamura Y, Hoffman GG, Toriello H, Smith LT, Byers PH, Greenspan DS. Order of intron removal influences multiple splice outcomes, including a two-exon skip, in a COL5A1 acceptor-site mutation that results in abnormal pro-alpha1(V) N-propeptides and Ehlers-Danlos syndrome type I. Am J Hum Genet. 2002; 71:451–65. doi: S0002-9297(07)60327-9 [pii] 10.1086/342099. [PubMed: 12145749]

Wang WL, Li Q, Xu J, Cvekl A. Lens fiber cell differentiation and denucleation are disrupted through expression of the N-terminal nuclear receptor box of NCOA6 and result in p53-dependent and p53-independent apoptosis. Mol Biol Cell. 2010; 21:2453–68. doi: 10.1091/mbc.E09-12-1031. [PubMed: 20484573]

Wawrousek EF, Chepelinsky AB, McDermott JB, Piatigorsky J. Regulation of the murine alpha A-crystallin promoter in transgenic mice. Developmental Biology. 1990; 137:68–76. [PubMed: 2295367]

Wenk M, Herbst R, Hoeger D, Kretschmar M, Lubsen NH, Jaenicke R. Gamma S-crystallin of bovine and human eye lens: solution structure, stability and folding of the intact two-domain protein and its separate domains. Biophys.Chem. 2000; 86:95–108. [PubMed: 11026675]

Wormstone IM, Tamiya S, Marcantonio JM, Reddan JR. Hepatocyte growth factor function and c-Met expression in human lens epithelial cells. Invest Ophthalmol Vis.Sci. 2000; 41:4216–4222. [PubMed: 11095618]

Wride MA, Sanders EJ. Nuclear degeneration in the developing lens and its regulation by TNFalpha. Exp Eye Res. 1998; 66:371–83. doi: 10.1006/exer.1997.0440. [PubMed: 9533864]

Yang Z, Li Q, Ma Z, Guo Y, Zhu S, Ma X. A G-->T splice site mutation of CRYBA1/A3 associated with autosomal dominant suture cataracts in a Chinese family. Mol Vis. 2011; 17:2065–71. doi: 225 [pii]. [PubMed: 21850182]

Yang Z, Su D, Li Q, Yang F, Ma Z, Zhu S, Ma X. A novel T-->G splice site mutation of CRYBA1/A3 associated with autosomal dominant nuclear cataracts in a Chinese family. Mol Vis. 2012; 18:1283–8. [PubMed: 22665976]

Yu Y, Li J, Xu J, Wang Q, Yao K. Congenital polymorphic cataract associated with a G to A splice site mutation in the human beta-crystallin gene CRYbetaA3/A1. Mol Vis. 2012; 18:2213–20. [PubMed: 22919269]

Zhu Y, Shentu X, Wang W, Li J, Jin C, Yao K. A Chinese family with progressive childhood cataracts and IVS3+1G>A CRYBA3/A1 mutations. Mol Vis. 2010; 16:2347–53. doi: 251 [pii]. [PubMed: 21139983]

Highlights

We investigated the mechanism of cataracts caused by a c.215+1G>A splice mutation in CRYBA1.

This mutation causes a splice defect in which the mutant mRNA skips both exons 3 and 4, escaping NMD.

This causes an in-frame deletion of the mRNA encoding an unstable p.Ile33_Ala119del protein.

The mutant βA3/A1-crystallin causes toxicity and degeneration of differentiating lens cells.

The mutant βA3/A1-crystallin acts by inducing the UPR culminating in apoptosis.

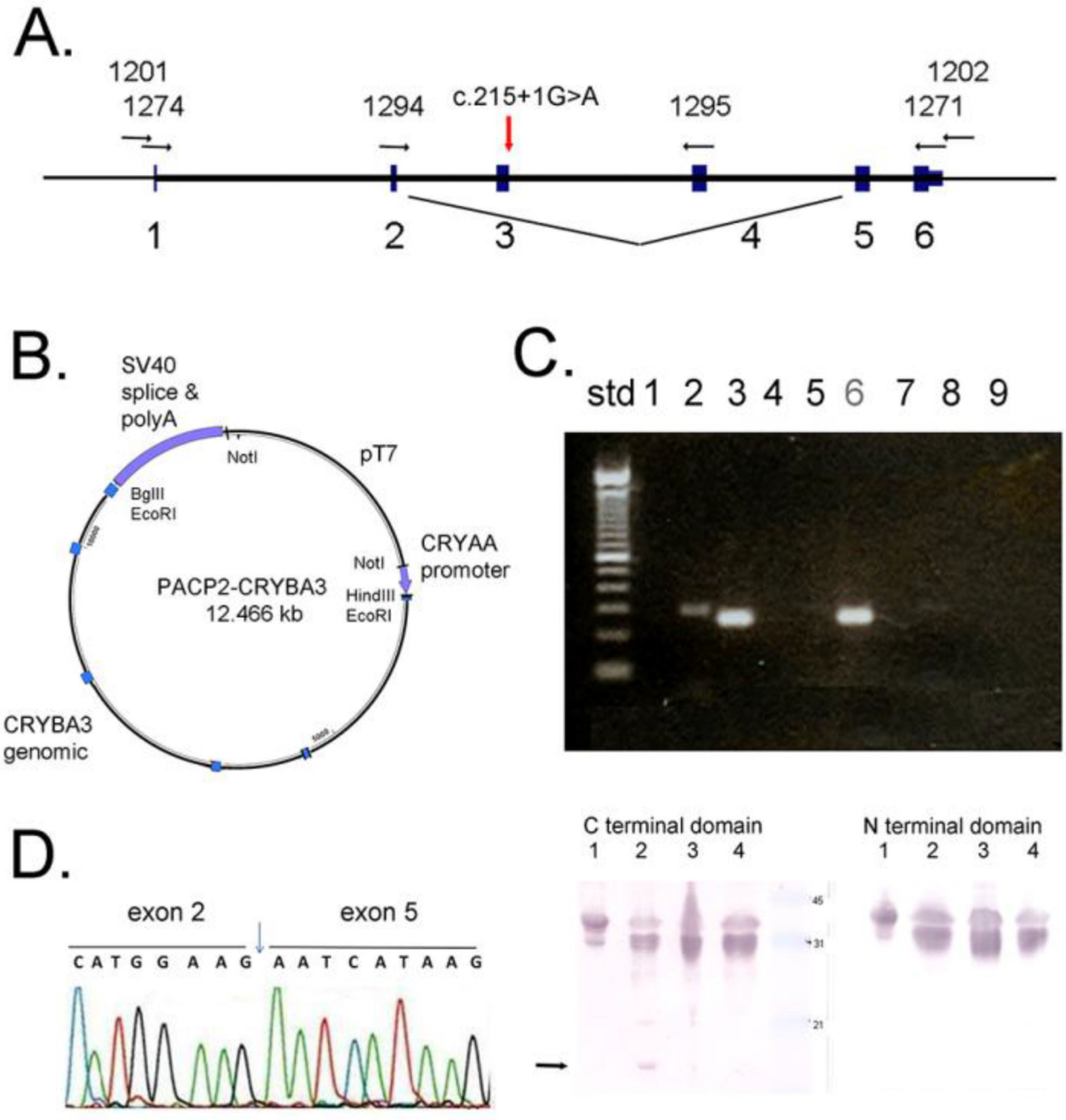

Fig. 1.

CRYBA1 and the c.215+1G>A splice mutation. A. Structure of the CRYBA1 gene, showing primer locations, the c.215+1G>A mutation, and its effects on splicing. B. Schematic drawing of the c.215+1G>A CRYBA1 or CRYBA1 PACP2 vector. It comprises the first 412 bp of the chicken αA-Crystallin promoter followed by the c.215+1G>A CRYBA1 or wt CRYBA1 genomic clone, and the SV40 T antigen splice site and polyadenylation signal in a PT7 backbone. C. RT-PCR Top. lane 1: transgenic lens mRNA, primers 1294/1295 (1295 is human specific, nts 54-301, exons 2-4), lane 2: transgenic lens mRNA, primers 1294/1271

(1271 is human specific, nts 54-596, exons 2-6), lane 3: transgenic lens mRNA, primers 1294/1297 (1297 is mouse specific, nts 54-301, exons 2-4); lanes 4-6, identical to lanes 1-3, but with control lens mRNA; lanes 7-9, identical but without template; Bottom, Western blot using antibody to C-terminal domain (left) and N-terminal domain (right). 1. Control lens extract, 2. Transgenic lens extract (OD05-0057), 3. Transgenic lens extract (OD05-0075), 4. positive control (recombinant βA3-crystallin) D. Sequence tracing of mutant mRNA showing junction of exon 2 and exon 5 sequence

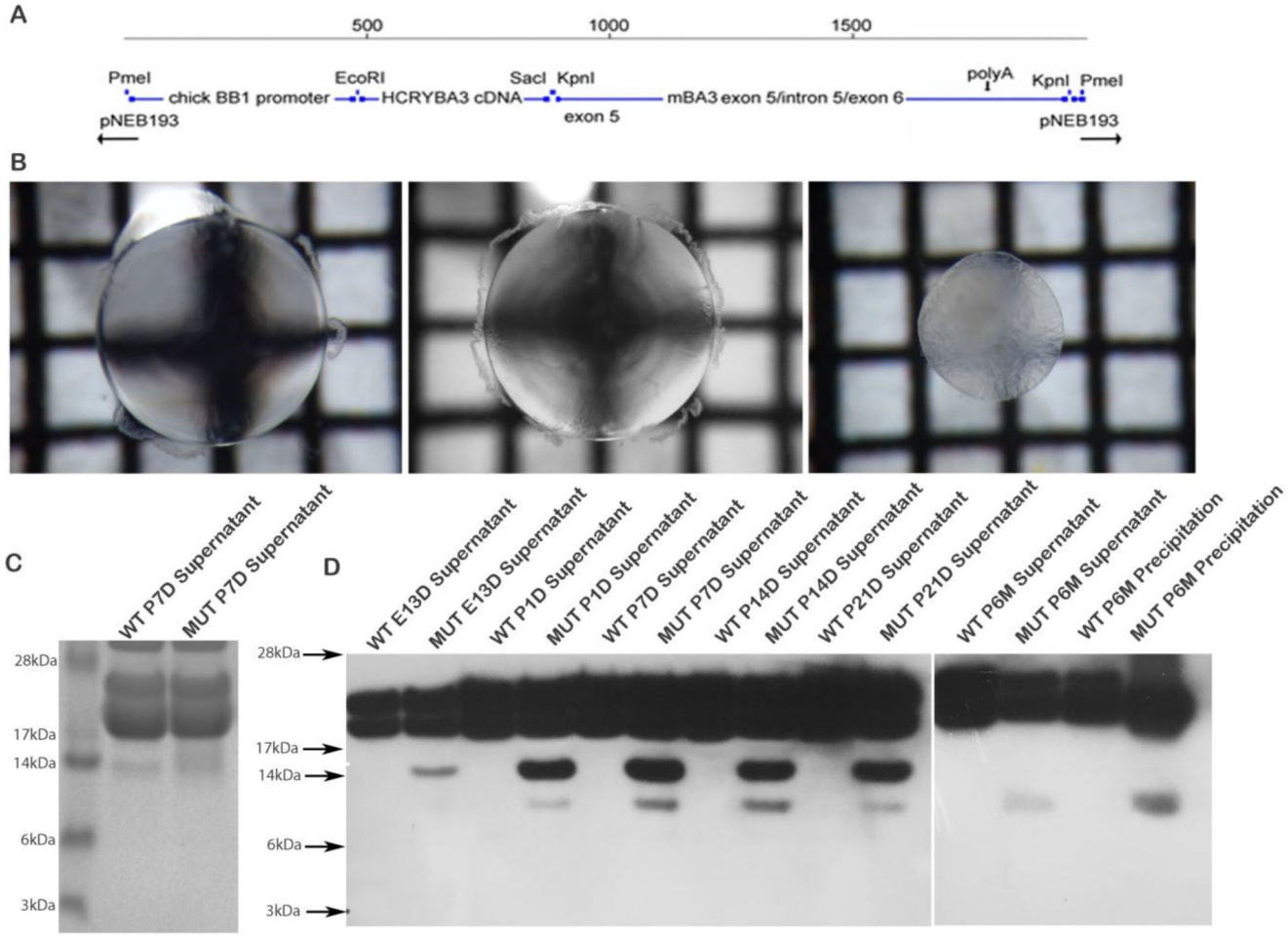

Fig. 2.

pCBB1/ c.97_357del CRYBA1 transgenic mice. A. Schematic diagram of the pCBB1/ c. 97_357del CRYBA1 construct vector containing the 468 bp chicken βB1-crystallin promoter followed by the cloning site with either the human CRYBA1 wt or c.97_357del CRYBA1 cDNA, and then the terminal part of mouse βa3/a1 exon5, intron5 and exon6, including the final splice site and the polyadenylation signal in a pNEB193 backbone. B. Gross morphology of lenses from wild type, CRYBA1 wt transgenic, and c.97_357del CRYBA1 transgenic mice. Left: wild type lens (P25W) showing no opacity; Center: CRYBA1 wt lens (P25W) showing no opacity; Right: c.97_357del CRYBA1 lens (P25W) showing opacity and some posterior polar bulging of the lens. The size of c.97_357del CRYBA1 lens was consistently smaller than the WT and CRYBA1 wt lenses. C. Polyacrylamide gel electrophoresis and D. Western blot analysis of lens soluble protein extracts and comparison to insoluble protein extracts from wild type and transgenic mice. Extracts of lens proteins were separated by 4–12% gradient NuPAGE. WT: wild type lens protein extracts, MUT: c. 97_357del CRYBA1 transgenic lens protein extracts. Western blots using a polyclonal antibody to a recombinant fragment corresponding to amino acids 1 to 215 of βA3-crystallin confirmed expression of endogenous βA3/A1-crystallin around 22 kDa and the mutant

βA3/A1-crystallin seen in extracts of transgenic mouse lenses around 14 kDa, with an additional band of apparently degraded mutant βA3/A1 protein at approximately 10 kDa

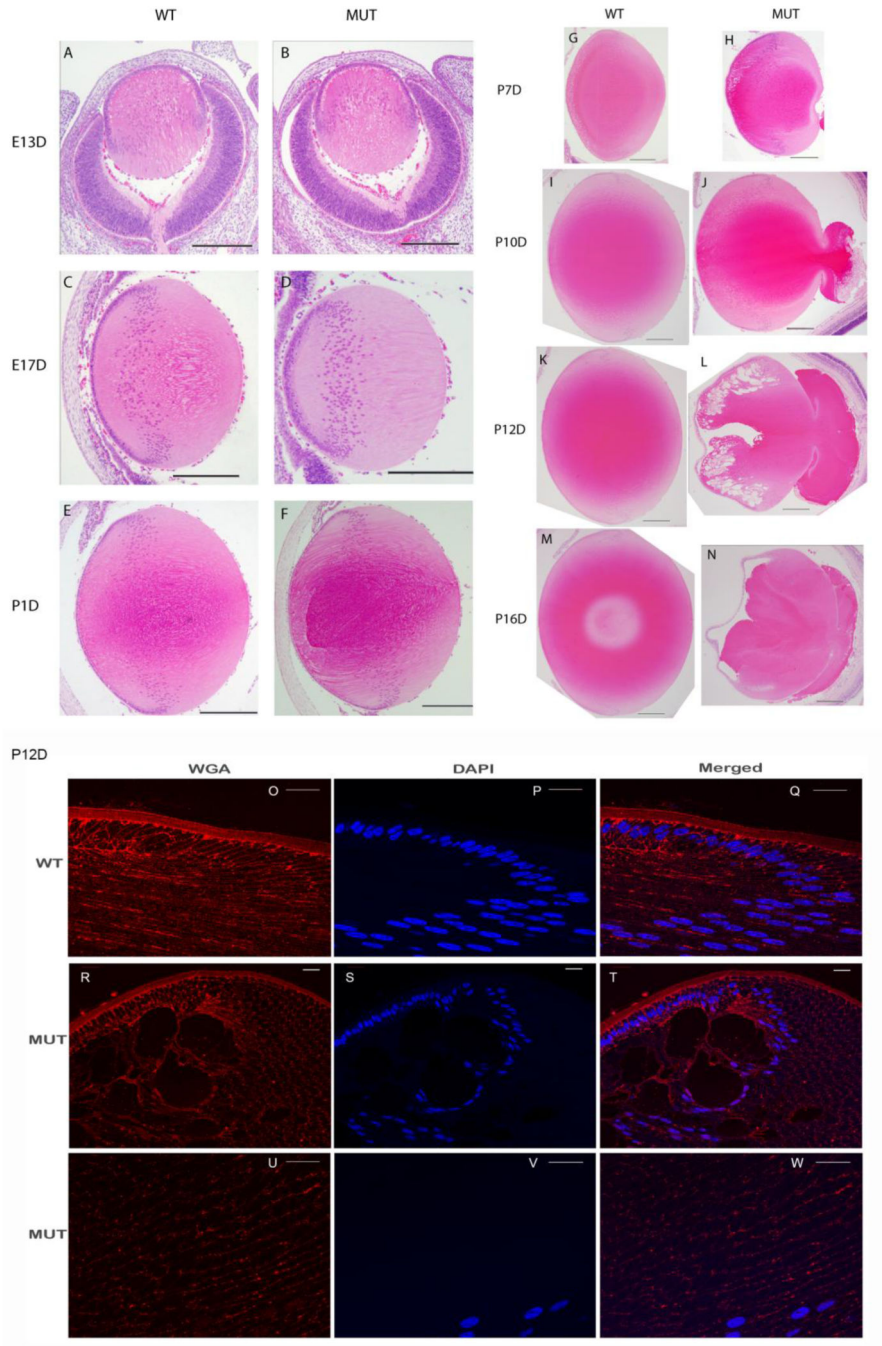

Fig. 3.

Micrographs of lenses from WT (A, C, and E) and HBA3/A1SPL (B, D, and F) transgenic mice. A and B are from 13 day embryos; C and D are from 17 day embryos; E and F are from postnatal day 1 mice. At each age, lenses from c.97_357del CRYBA1 mutant mice appeared similar to those of WT mice.. Histology of lenses from WT (G, I, K, and M) and c. 97_357del CRYBA1 (H, J, L, and N) transgenic mice at P7D (G, H), P10D (I, J), P12D (K, L) and P16D (M, N) respectively. P7D, lens began to exhibit abnormalities in a few severely affected mice (G, H), including vacuolated equatorial fiber cells, especially beneath the

anterior epithelia, and disorganized fiber cells. Posterior capsular rupture was earliest detected at P10D (I, J). With or without capsular rupture, severely damaged lens fiber cells were seen in essentially all mice at P12D, with fiber cells showing large vacuoles merging to form extracellular lacunae, and the cortical fiber cells detached from anterior epithelia (K, L). Scale bars for Fig. 3A-N are 100μm In addition, by P16D (M, N), lens fiber cells in c. 97_357del CRYBA1 transgenic mice showed defective fiber cell elongation, migration, alignment, and denucleation distinctly different from those in WT lenses. Details of the lens fiber cell morphology can be seen in O-Q (wt, 40×), R-T (mutant transgenic, 20×), and U-W (mutant transgenic, 40×), where the wt fibers appear as long gracile strands aligned with the axis of the lens. The c.97_357del CRYBA1 transgenic mouse lenses show lacunae, but also thickened fiber cells stretched apart and in some disarray, with some fiber cells oriented vertically to the lens axis (shown by the nuclei in the figures) so that they appear in cross section as hexagonal shapes (especially visible in the 20×, (R-T). Scale bars for Fig. 3N-W are 10 μm.

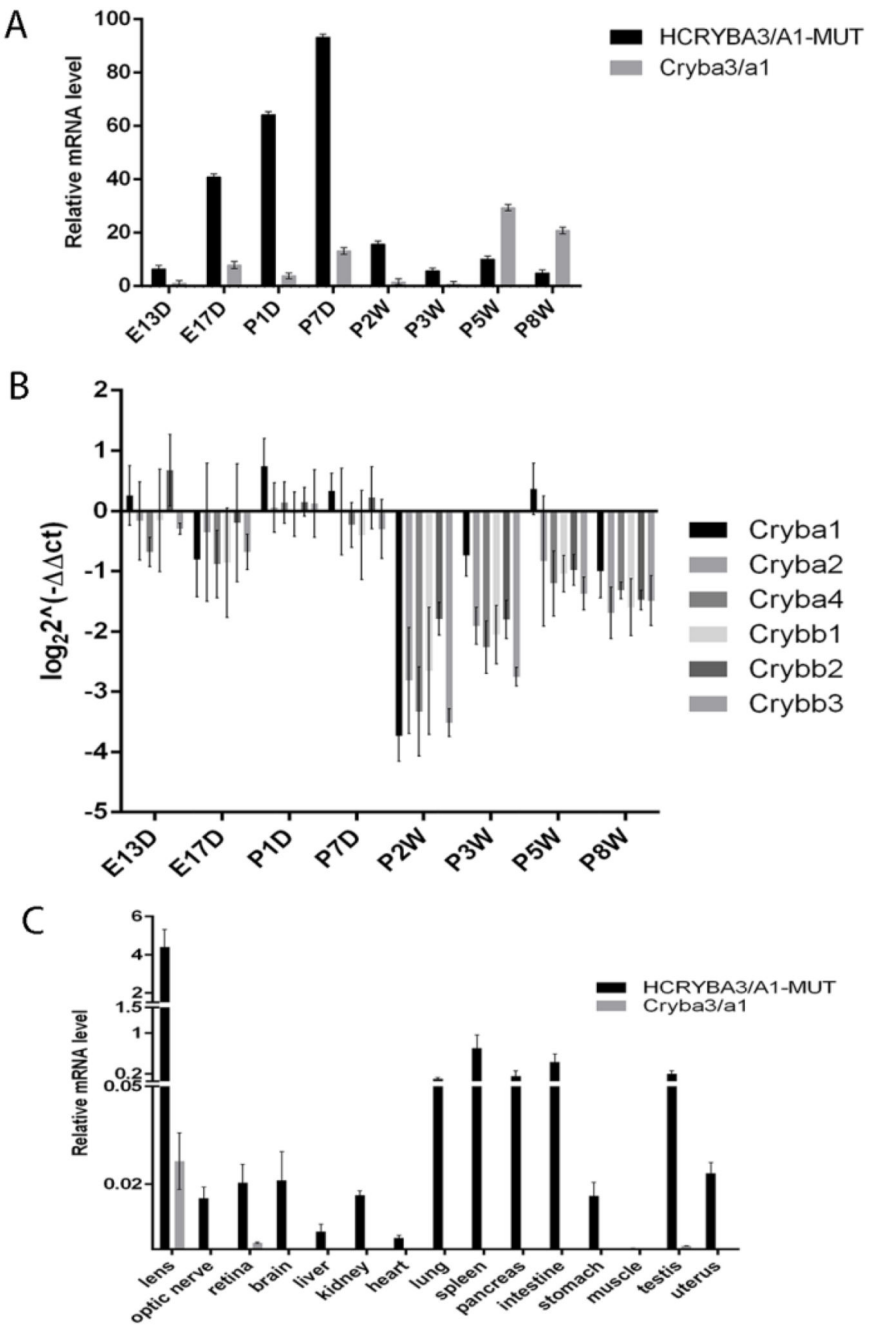

Fig. 4.

Expression analysis of β-crystallin at different ages and in different tissues by quantitative Real-Time PCR. GAPDH transcript was used as an endogenous control. A: c.97_357del CRYBA1 mutant and endogenous Cryba1 expression during mouse lens development. B: expression differences in expression of β-crystallins between c.97_357del CRYBA1 mutant and WT mice during lens development. ΔΔCT values are shown, so that a value of 0 indicates no change. C: c.97_357del CRYBA1 mutant and endogenous wt CRYBA1 mRNA expression in different mouse tissues

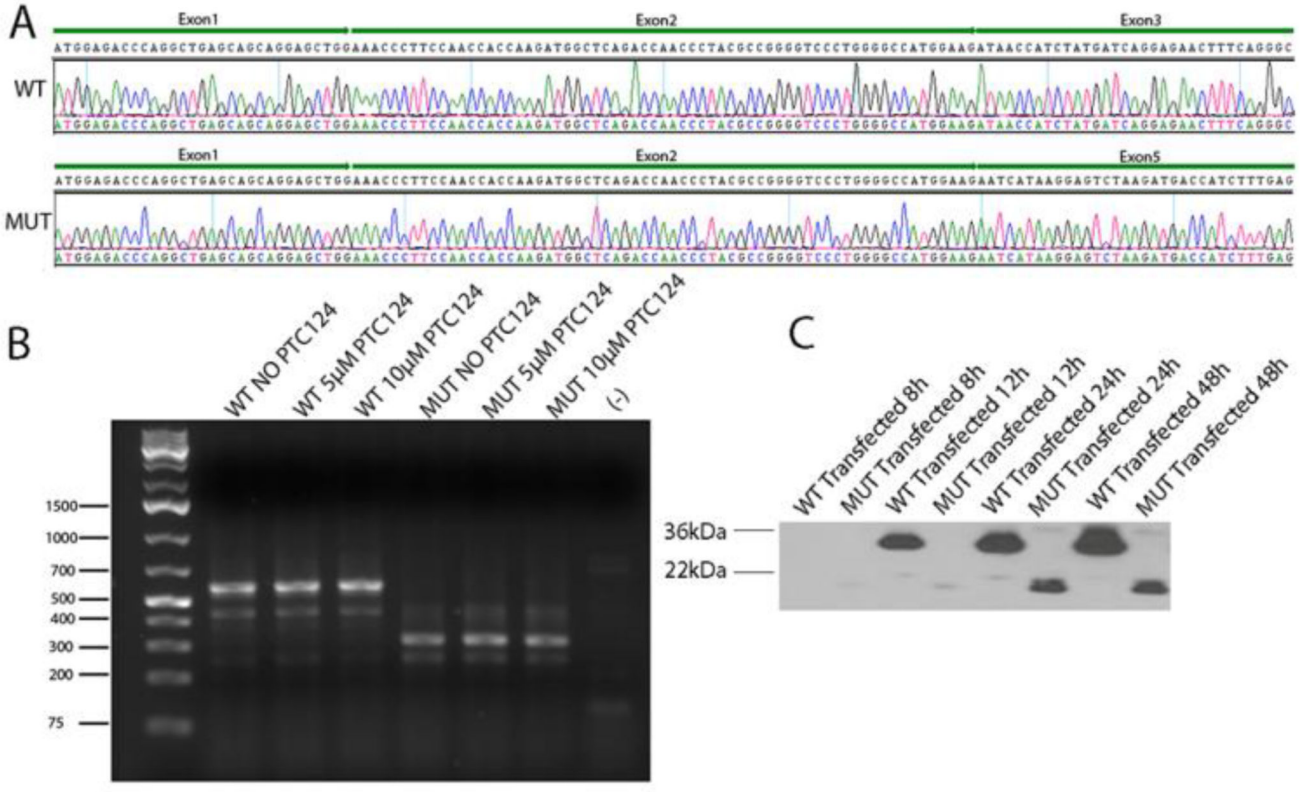

Fig. 5.

Transcription analysis of the CRYBA1 gene. A: sequence tracings of wild and mutant transcript, with the mutant transcript indicating that exons 3 and 4 were skipped. B: RT-PCR products separated on a 1% agarose gel. Products from HLE cells transfected with pcDNA4A/CRYBA1/WT showed a correct 572 bp band; while cells transfected with pcDNA4A/ c.215+1G>A CRYBA1 showed a band around 300bp. There was no extra product under treatment with PTC124. C: Western blot of transfected cells at different times

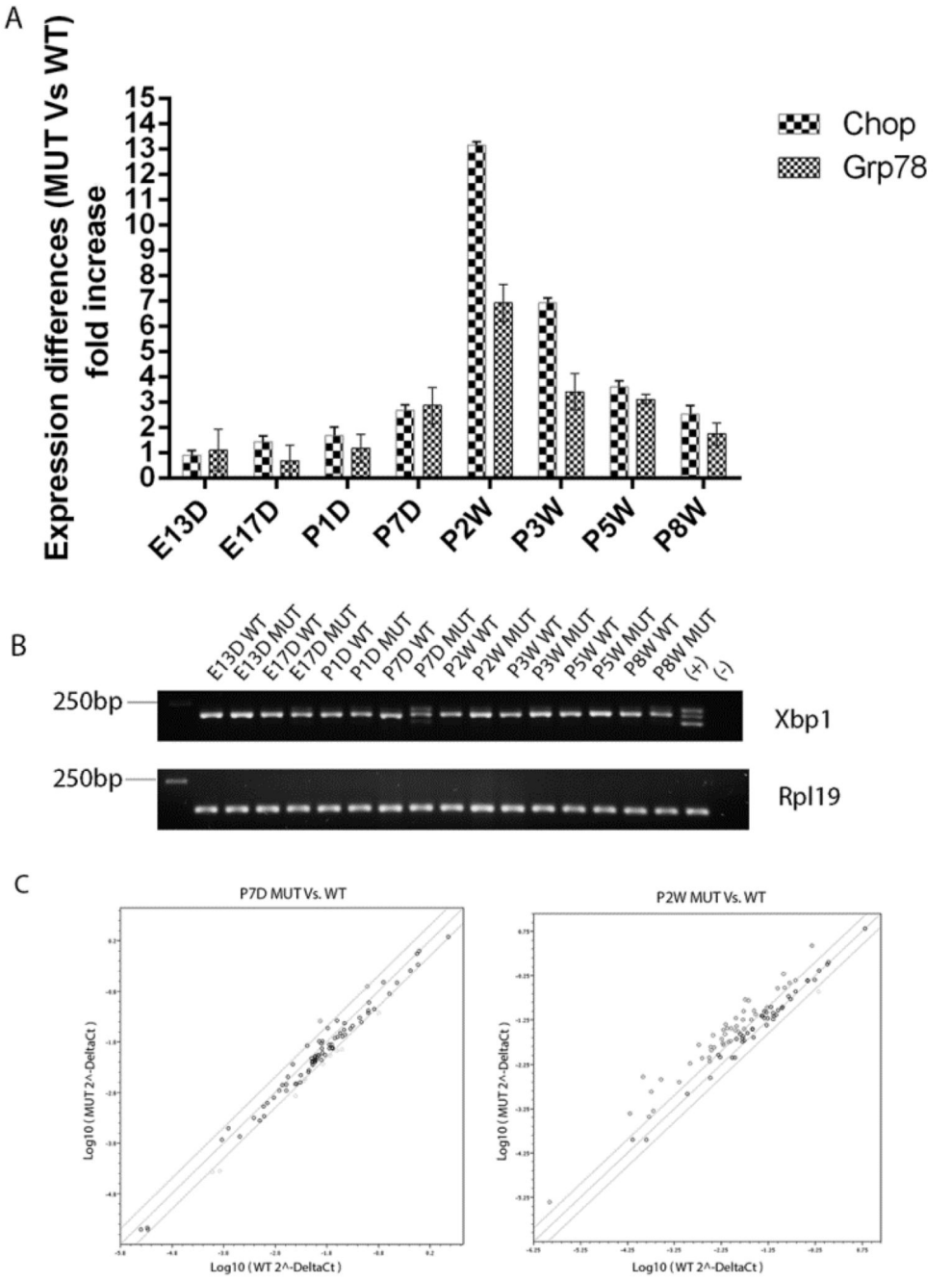

Fig. 6.

Unfolded Protein Response activation. A: Expression of BiP and pre-apoptotic factor CHOP. Rpl19 was used as an endogenous control. Their expressions were increased significantly, peaking at P2W. B: Xbp1 splicing detection. Spliced Xbp1 was exhibited at P7D when mutant CRYBA1 expression peaked. C: Comparison of UPR and apoptotic pathway gene expression in mouse lenses transgenic for c.97_357del cDNA and WT CRYBA1 at P7D and P2W. Lines show twofold × expression differences

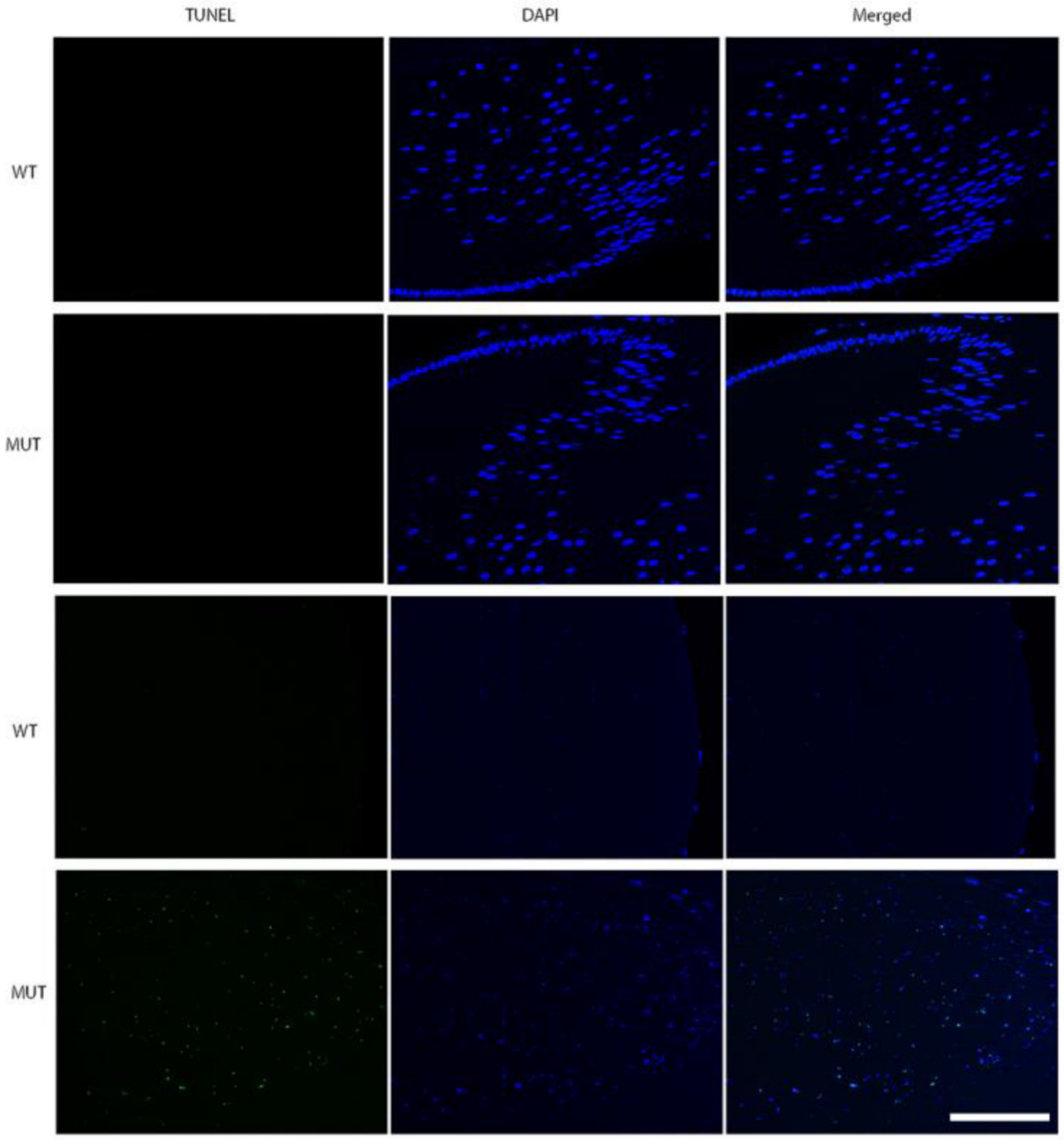

Fig. 7.

Confocal micrographs of P10D transgenic mouse lens sections stained with DAPI (blue) and TUNEL Apoptosis Detection Kit (green). Top two panels: cortical bow region of the lens. Bottom two panels: posterior pole of the lens. TUNEL positive cells were detected in the posterior nucleus of c.97_357del cDNA but not WT CRYBA1 transgenic mouse lenses, and was absent from the cortical bow region of both. Scale bar, 50μm

Table 1

Primer list

M-cryba1-F	GTTGGTTCAACAATGAAGTT
M-cryba1-R	GCGTGAGATCCCCACTCTGG
M-cryba2-F	GGGAGACTATCCTTGCTGGAG
M-cryba2-R	GGAAGTTTTCCCCCTCAAAC
M-cryba4-F	CCATCTTCGAGCAGGAGAAC
M-cryba4-R	CCAGGAAACTGGGAACAAAC
M-crybb1-F	GACACCTGGACCAGCAGTTA
M-crybb1-R	ATGGTGTTGCCCTTGAAGTT
M-crybb2-F	CCCCAACTTTACTGGCAAGA
M-crybb2-R	CGGTAGCCAGGGTACTGGT
M-crybb3-F	CCTCCAGTTTGAGGCAGAAG
M-crybb3-R	GCTTGCCCTGGAAGTTCTCT
M-Xbp1-RT-F	AGGCAACAGTGTCAGAGTCC
M-Xbp1-RT-R	gaaccaggagttaagaacacg
M-Chop-qrt-F	GAATAACAGCCGGAACCTGA
M-Chop-qrt-R	ACACCGTCTCCAAGGTGAAA
M-Grp78-qrt-F	CAGATCTTCTCCACGGCTTC
M-Grp78-qrt-R	AGCAGGAGGAATTCCAGTCA
M-Rpl19-qrt-F	AGCCTGTGACTGTCCATTCC
M-Rpl19-qrt-R	TCATCCAGGTCACCTTCTCA
HCRYBA1_f	TCGCCGAATCCAACAGTAG
HCRYBA1_r	TCCAGGGTACTGGTAGCAAA
CRYBA3_KPN1_F	cggGGTACCtatggagacccaggctgagcagcaggagctg
CRYBA3_BamH1_R	cggGGTACCcaagccccagactccctcgtaac
CRYBA3_BamH1_F	cggGGTACCtggcatggctggctgtttggcc
CRYBA3_Xba1_R	cggTCTAGAccaatggacaggccaaggacttatg
CRYBA3_Xba1_F	cggTCTAGAtattatccctggcagaccatttc
CRYBA3_Nde1_R	cggCATATGcacggaagtggaaatttcagagac
CRYBA3_Nde1_F	cggCATATGagggatgggacaagagggtgtggac
CRYBA3_Xho1_R	cggCTCGAGctactgttggattcggcgaatcgattgg